심리학석사학위논문

Specificity of surround interaction for global motion directionality in awake monkey V1

원숭이 일차시각피질의 주변상호작용의 특정성에 기초한 광역운동 방향선택성

2014 년 2 월

서울대학교 대학원

심리학과 생물심리 전공

김 은 영

Abstract

Specificity of surround interaction for global motion directionality in awake monkey V1

Kim, Eunyoung
Department of Psychology
The Graduate School
Seoul National University

Neurons of the primary visual cortex (V1) process visual information presented within the classical receptive field (cRF), and this local information is thought to be integrated with that outside the cRF to recover global visual features in later stages. However, it has been known that even in the V1, neuronal activity is modulated by stimuli outside the cRF. In line with this, it was reported that V1 neurons are modulated by temporal interval of spatiotemporal stimulus sequence extending beyond the cRF (Kim et al., 2012), suggesting that V1 neurons participate in processing stimulus motion extending beyond the cRF – global motion.

In the current study, we tested the hypothesis that V1 neurons have directional preference for global motion extending beyond the cRF, and that this is based on fine-tuned surround interaction. Specifically, we measured ***global directional preference*** with a sequence of two focal stationary Gabor stimuli; the preceding one (S1) presented

outside the cRF and the following one (S2) presented inside the cRF with a stimulus onset asynchrony (SOA) of 50 or 100ms. The S1 stimulus appeared at either flanking sides of the cRF before the S2, thus making two directions of stimulus sequence. And this was compared with ***local directional preference*** that we measured with a Gabor stimulus confined within the cRF that drifted along two directions orthogonal to preferred orientation.

Although the S1 alone did not evoke spiking responses, the response to the S2 was significantly modulated by the S1, consistent with the previous study (Kim et al., 2012). The magnitude of modulation was asymmetrical between the two sequence directions, indicating that the cells showed a direction preference for apparent motion consisting of S1 and S2 that extended beyond the cRF. There was a significant positive relationship between global and local directional preferences, suggesting that V1 neurons tend to prefer the global motion direction that matched with their local directional preference. This positive correlation was significant for SOA of 50ms, but not for 100ms. These results suggest that V1 neurons participate in processing global motion based on surround interaction that is fine tuned for spatial and temporal relations between center and surround stimuli.

Keywords: surround interaction, receptive field, V1, global motion, directionality, aperture problem

Student Number: 2011-20118

Contents

Tables

Figures

1. Introduction

Information regarding visual events is broken into small pieces of local information by sensory neurons, and a fundamental role of central visual system is thought to integrate this local information to derive a meaningful percept. Understanding how various aspects of visual information are encoded by sensory neurons and combined later to guide visual behaviors is a great challenge in science.

The neurons of primary visual cortex (V1) are selectively activated by the stimuli presented within their receptive field (RF). Also, V1 neurons have been regarded as local motion energy filters that analyzes the motion of 1-D patterns, whereas the neurons of medial temporal lobe (MT) can process motion information of complex patterns such as 2-D patterns (Movshon et al., 1986). Furthermore, V1 neurons are faced with the 'aperture problem' (Marr, 1982) (Figure 1). Since this problem is closely related to the small size of the RF of V1, some of researchers asserted that the integration of global motion information may be processed in the cortical areas downstream to V1 such as the area MT that contain cells with large RFs (10 times larger than those in V1) and well-developed direction selectivity column (Dubner and Zeki, 1971; Albright, 1984; -reviewed in Born and Bradley, 2005).

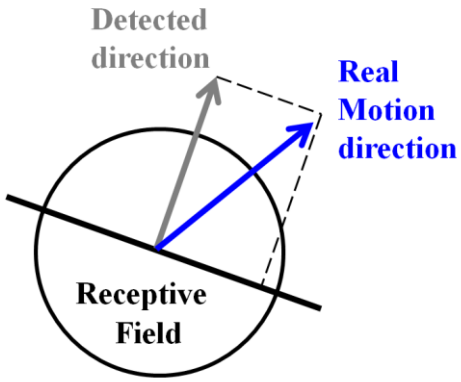

Figure 1. Aperture problem of single V1 neuron. If a moving line is seen through a small aperture, the direction of its motion is ambiguous – aperture problem. The RF size of V1 neuron is small and traditionally, V1 neuron is thought to be faced with such a problem. In this figure, even though the real direction is 'blue', the detected direction through the aperture, or by the RF of single V1 neurons is 'gray' which is always orthogonal to the orientation of stimulus line. Therefore, the information regarding global motion outside the RF is unavailable in the activity of V1 neurons. Throughout this thesis, local motion means motion extracted by small classical receptive field (cRF), and global motion means motion extending outside the cRF.

However, recent studies reported that the information regarding global motion is not available in the activity of MT neurons (Majaj et al., 2007; Hedges et al., 2011). According to Majaj et al. (2007), motion signals are not pooled across the entire RF, so the RF of MT cell is not the unit of motion integration even within the RF. In another study (Hedges et al., 2011), a global motion direction that was made of local motion pulse across the RF did not modulate spiking responses in a way consistent with MT's processing of global motion, and spiking responses of the MT were determined entirely by the local motion directions. Thus, the anatomical site of signal integration for global motion is obscure.

On the other hand, new properties of the V1 neurons have been reported that suggest the roles of the V1 for global motion processing. End-stopped V1 neurons can process motion information unambiguously (Pack et al., 2003). The neural responses to cRF target are significantly modulated by the context, as in RF surround or center-surround relationship about the properties such as contrast, orientation, and direction (Cavanaugh et al., 2002; Series et al., 2003). Also, from the anatomical perspective, lateral and

feedback connections enable V1 neurons to process motion information which temporally and spatially distributed (Young, 2000). Another study that is closely related to the issue of potential global motion processing by the V1 neurons was done by Kim et al. (2012). They showed that the spike response of V1 neurons was modulated by temporal interval and direction of spatiotemporal stimulus sequence extending beyond the cRF. In addition, a study by Guo et al. (2006) showed that in 25 of 81 recorded V1 neurons, the activity was significantly modulated by different global directions of continual bar stimulus.

These studies suggest the possibility that V1 neurons may participate in processing stimulus motion extending beyond the cRF. In the current study, we examined the possibility, and specifically tested the hypothesis that fine-tuned surround interaction gives a rise to directional preference for motion extending beyond the cRF (Figure 2). We determined directional preference with a sequence of two focal stationary Gabor stimuli, the preceding one (S1) outside the cRF and the following one (S2) within the cRF (global directionality), and compared it with directional preference determined with drifting Gabor stimuli confined within the cRF (local directionality). Surround stimuli do not evoke spike response by themselves, but evoke subthreshold intracellular response (Bringuier et al., 1999). Our hypothesis is that surround zone is inhomogeneous in evoking the subthreshold response, and when this interacts with intracellular potential changes evoked by the RF stimulus, intracellular potential will differ depending on which part of surround zone was stimulated. When these different intracellular potentials undergo a threshold mechanism (Priebe and Ferster, 2008), a different spike response will result, revealing an asymmetric response depending on stimulus direction.

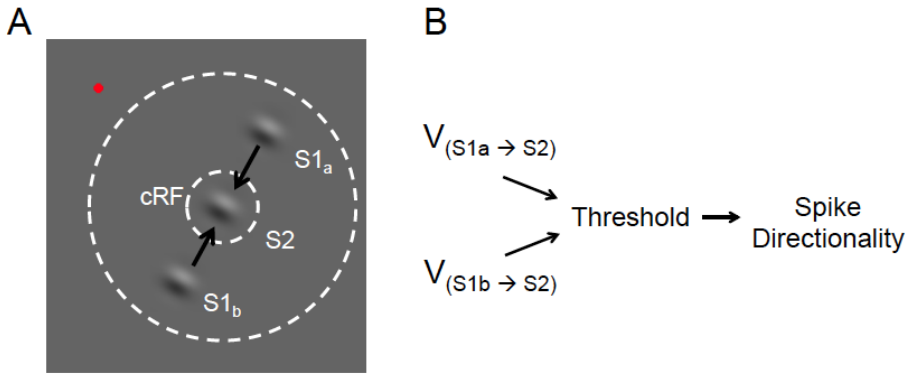

Figure 2. Logic of experiment. A. Spatial layout of stimulus condition. Red dot is fixation point, inner dashed circle is boundary of classical receptive field (cRF), and outer dashed circle is zone of surround. Important assumption is that surround zone is not homogeneous in modulating the cell response to RF stimulus. Local motion is a motion within cRF, and global motion is one extending both inside and outside the cRF. We used apparent motion stimulus in which two stimuli were sequentially presented with a temporal asynchrony, the first one (S1) outside the cRF and the second one (S2) within the cRF. S1 can be presented at various locations in surround zone. Here, two positions, a and b, are shown. **B.** Intracellular voltage change following two stimulus sequence (S1a->S2 and S1b->S2) undergoes a threshold mechanism to be expressed as spike activity. S2 was always the same and presented within cRF.

The goal of experiment was to determine whether two stimulus sequences in opposite order evoke different spike response. And if so, how the directional preference for sequence stimulus relates to the cell's directional preference for motion confined within the cRF.

2. Method

2.1. Subjects

Two adult male macaque monkeys (DC, IR) were used for the current study (Table 1). All surgical preparations and experimental procedures were approved by the Seoul National University Animal Care and Use Committee, and complied with the Guidelines of the National Institutes of Health of the United States. These animals had been used for other experiments involving extracellular recording and behavioral tasks prior to the current study.

Name	Species	Sex	Age (year)	Weight(kg)	Experimental state
DC	Macaca mulatta	Male	11	7	Awake
IR	Macaca fascicularis	Male	11	7.56	Awake

Tablel. Subject profiles

2.1.1. Surgical procedures

In order to affix a head-post for achieving a head-restraint condition and two recording cylinders for allowing passage of electrodes, an aseptic surgery was performed under anesthesia. This was aided by high pressure steam or EO-gas sterilization and a clean room supplied with HEPA-filtered air. Animal feeding was restricted on the day of surgery for preventing vomiting and choking under anesthesia. Animals were initially tranquilized with an intramuscular injection of ketamine hydrochloride (0.5ml/kg) and an injection of atropine sulfate (0.1-0.2ml) was given to maintain the clear respiratory track.

Then, surgical anesthesia was induced and maintained with sodium thiopental (about 0.2ml, every 15 minutes) through a cathether (22-24 gauge) into a blood vessel in the hind leg. The body temperature was maintained at around 37 degrees using a regulated heating pad (TR-200, Fine Science Tools). The head was shaved, cleaned with povidone-iodine solution, and fixated on a Horsely-Clarke stereotaxic frame (David Kopf). The skull overlying the operculum of the primary visual cortex (V1) was exposed and cleaned, and two custom-designed recording cylinders made of titanium alloy (outside diameter = 20mm, height = 10mm) were affixed to the skull with the aid of titanium screws (Adams et al., 2007). The position of the two cylinders was aimed posterior to the lunate sulcus but anterior to occipital margin of the bone sutures overlying both opercula. A cylindrical head-post made of titanium alloy with an outer diameter of 20mm was also affixed typically at AP=-10mm, ML=0mm. In order to aid fixture of the head post and recording cylinder to the skull, a bone cement (Palacos R, Biomet Merck Cementing Technologies AB, Sweden) was mixed with additional antibiotic powders including Vancomycin, Cefazolin sodium, and Kanamycin, and applied around the screws and recording cylinders.

2.1.2. Behavioral training: Fixation and saccade tasks

After recovery from the surgery, the subjects underwent behavioral training sessions of about 2-3 weeks before the start of main experiments. During training and subsequent recording sessions, access to water was restricted during weekends to motivate the subjects to participate the task more actively. The goal of the current study was to determine receptive field (RF) properties of single V1 neurons in awake monkeys, and for this, the subject was required to maintain fixation while visual stimuli were presented at the RF. Thus, the monkeys were first trained with a simple fixation task in which they maintained their eyes on a central point within a window of 1.6-2 deg for various

durations (300/500/700ms) for a liquid reward. After the subjects were trained for this, a Gabor stimulus explained below was additionally presented at an eccentric location for a brief period (from 20 to 800ms depending on experimental conditions) of time, and their task was to maintain central fixation and to ignore the stimulus in periphery. After successful fixation for required duration, another point stimulus was presented ±3.5 deg away from the central point as a saccadic target. The reward was contingent on successful fixation at central target, subsequent saccadic eye movement toward the saccadic target, and maintenance of fixation at the saccadic target for additional 100ms. This visual task is very natural for monkeys and so, they readily performed the task without any difficulty.

2.1.3. Craniotomy and dura cleaning

After the subjects became familiar with the behavioral task explained above, a craniotomy was performed under ketamine tranquility. A small piece of skull inside the recording cylinder, typically about 2-3mm in diameter, was removed for electrode passage, and the dura was exposed. The skull-removed region was covered with antibiotic ointment and the whole area inside the cylinder was protected with a sterilized threaded Teflon cap and a ring gasket sealing the junction between the cap and cylinder surfaces. As the dura mater thickened and soft fibrous structure grew over exposed dura with the lapse of time, the dura was thinned under ketamine tranquility (ketamine hydrochloride, 0.5ml/kg) with the aid of microscope. This was to facilitate the electrode penetration of the dura and thus to minimize tissue drag during its penetration, which otherwise increases an error in electrode depth reading.

2.2. Experiment environment

2.2.1. Computer system

There were two computers in the experimenter's zone; one was a stimulation computer that controlled all of visual stimulus presentations and eye calibrations. The other one was a data acquisition computer that recorded neuronal activities, eye position, and the output from a photodiode directly registering stimulus timing from the stimulus monitor. These two computers were connected by a network in TCP/IP. The subject faced a 24-inch CRT monitor (Sony GDM-FW900, 100Hz, 800 X 600 pixels) at a distance of 77 cm. The diode output was used to verify the accuracy of stimulus timing, and those trials with stimulus timing deviating from the intended were eliminated during off-line analysis (Figure 3).

Valid trial

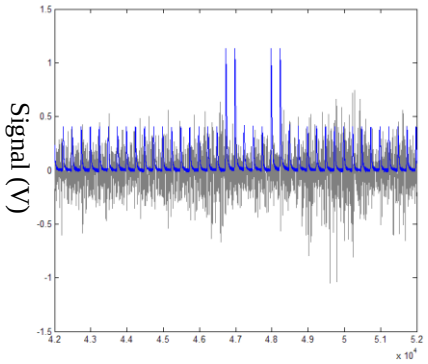

Invalid trial

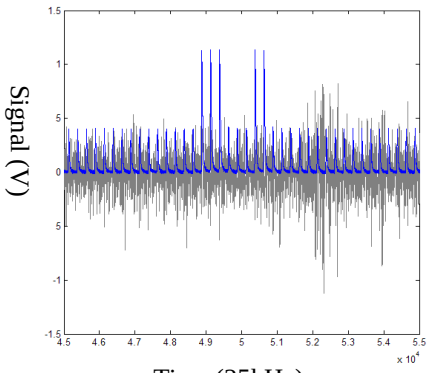

Timing information

Celldata

Field	Value
iSpike_25	<24x1 double>
iSpike	<24x1 double>
Waveform	<24x30 double>
fr	<2x3194 double>
Photo1kHz	<1x3194 double>
Eye	<2x3194 double>
Pupil	<2x3194 double>
StimOn	[1866;1876;1916;1926]

Timing information

Celldata

Field	Value
iSpike_25	<69x1 double>
iSpike	<69x1 double>
Waveform	<69x30 double>
fr	<9x3358 double>
Photo1kHz	<1x3358 double>
Eye	<2x3358 double>
Pupil	<2x3358 double>
StimOn	[1952;1962;1972;2012;2022]

Figure 3. Examples of valid and invalid trials (#20120618 : t_1_1.daq, t_1_104.daq). Blue: photodiode output. Gray: neural signal. In valid trial, we presented sequential stimulus for 40ms (20ms, each). Therefore, the number of photodiode was 4. (10ms for one diode)

2.2.2. Stimuli

A Gabor Stimulus was displayed on a gray background with a mean luminance of 5.85 cd/m^2. The Gabor stimulus used in this study was generated by two steps. First, a sinusoidal grating was made with sine and cosine functions, which specified in the formula (1). In this formula, x and y were visual angles (deg). The k represents a spatial frequency term in the unit of radian. θ was a orientation value in the unit of radian.

$$\textbf{Grating (x,y)= sin (kx·cos}\theta\textbf{ + ky·sin}\theta\textbf{)} \quad \text{- (1)}$$

Second, this sinusoidal grating was smoothed by Gaussian filter that represented as a formula (2). By changing the value of σ, we can manipulate the width of the Gaussian filter. In this study, we smoothed the sinusoidal grating with σ =1/4 of diameter of grating. We converted the grating to Gabor patch, by filtering with GaussFilter specified in the formula (2).

$$\textbf{GaussFilter (x)} = \frac{1}{\sigma\sqrt{2\pi}}\mathbf{e\text{^}}(-\mathbf{x^2}/\mathbf{2\sigma^2}) \quad \text{- (2)}$$

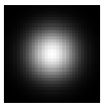

In experimental sessions, we always used a Gabor patch that had their optimal parameters (orientation, position, size, spatial frequency, temporal frequency). There were six experimental conditions, 4 for measuring global directionality and 2 for measuring local directionality. Additional 3 conditions were control conditions.

Measuring global directionality was accomplished by presenting sequential Gabor stimuli that encompassed inside and outside the RF. S1 refers to the target presented outside the RF, and S2 refers to the target presented inside the RF. Figure 3 shows three spatial layout examples from three different recording sessions. There were two possible global directions, [S1a-S2] and [S1b-S2] with two SOAs (50 or 100ms). By manipulating the temporal interval between S1 and S2 onsets and the position of S1, we created apparent motion stimuli that have two different directions with two different speeds.

Measuring local directionality was accomplished by presenting drifting Gabor stimulus inside the RF. There were two possible local directions orthogonal to the orientation of the Gabor stimulus. And the speed of drifting Gabor stimulus was the preferred temporal frequency of each recording session.

Figure 4. Stimulus arrangement for three example recording sessions. Each gray rectangle represents a part of the computer monitor that the subject was viewing. The red point is a fixation target (0.25° x 0.25°) that appeared at the center of monitor. White-dashed circle indicates the boundary of receptive field (RF). A stimulus that appears this region is called 'S2' target. If the same Gabor target appears at two flanking side of the RF, we called these as 'S1' target, and put 'a' or 'b' depending on its location. S1 target is always located on the surround region, 1.5 RF diameters away from the RF. **Left:** The optimal orientation of stimulus was 150 degrees. The spatial frequency was 1 cycle/deg, and the diameter was 1.6 degrees. **Middle:** The optimal

orientation of stimulus was 90 degrees. The spatial frequency was 1 cycle/deg, and the diameter was 2 degrees. **Right**: The optimal orientation of stimulus was 0 degrees. The spatial frequency was 4 cycles/deg, and the diameter was 1 degrees.

2.3. Measuring eye signal

Eye positions were measured with a camera (ET-49, 230Hz, Thomas Recording, Germany). The data acquisition computer sampled the voltage signals related to the eye positions provided by the camera at the rate of 25 kHz. During off-line analysis, the eye positions signals were down-sampled to 1000 Hz and smoothed with a 50-point moving average. In order to calibrate horizontal and vertical eye positions before starting training or main session, the voltage signal from the camera was converted to the degrees of visual angle.

$$H_{degree} = a\,H_{voltage} + b \qquad - \quad (3)$$
$$V_{degree} = c\,V_{voltage} + d$$

In the equation (3), a and c are gains, and b and d are offsets of two eye positions. For determining the value of gain and offset, we trained the monkey to fixate on a target presented on the monitor. In this fixation task, we presented a point stimulus that sequentially jumped every 1 sec in horizontal (-10, -5, 0, 5, 10) and vertical (-5, 0, 5) axes. If the eye entered an electronically-defined window about the stimulus (0.5~2 degrees), the monkey was rewarded with a few drops of juice. We obtained the exact horizontal and vertical offsets, by pressing a keyboard letter ‘o’ when the eye and target were aligned. These calibration methods are based on the assumption that the relationship between the output voltage and angular gaze direction is linear (4), which is valid within the central

visual space of about 10 deg.

$$\mathbf{Gaze}_{\mathbf{degree}} = (\mathbf{Signal}_{\mathbf{voltage}} + \mathbf{Offset}) \times \mathbf{Gain} \quad - \quad (4)$$

2.4. Measuring neural signal

2.4.1. Electrophysiological procedures

We recorded extracellular single and multi-unit activities using a microdrive (5-CH Mini-matrix system, Thomas Recording, Germany). We typically used two electrodes in one session (Quartz-platinum/tungsten electrode, Thomas Recording, Germany). In order to preventing bacterial infection, we cleaned the tip of electrode with distilled water and alcohol before starting each recording session. Since we set the tip of electrode flush with the tip of guide tube (electrode depth=0μm), we can estimate the relative depth of electrode during recording session. While the monkey was seated and its head was restrained onto a cross bar firmly fixed to the monkey chair (Macaque Restrainer, Primate Products, USA), the electrode guide tubes were lowered until the tip of guide tube touched the surface of the dura mater. An agarose solution (Agarose LE, SeaMatrix, Korea) was cooled below 36 degrees Celsius and applied around the guide tubes to help recording stability and electrode protection. Neural signals were pre-amplified with the gain of 20 (em112/R, Thomas Recording, Germany). Then, these signals were further amplified with the gain of 250-1000, and band-pass filtered with 500 Hz-20 kHz (MAF-05, Thomas Recording, Germany). The amplified neural signals were digitized at the rate of 25 kHz with a 16 bit precision.

2.4.2. Extracting Spikes

Spikes were extracted from raw extracellular potentials according to several criteria. By differentiating the raw potentials, we found the slope of the potential and the times of zero-crossing that the value of time differential goes from positive to negative or from negative to positive. They represent upper and lower peaks of spike-like potential. If the times of zero-crossing of a spike-like potential (upper or lower peak) exceeds the thresholds, it was extracted as a valid peak (Figure 5).

Upper threshold - the minimum value of voltage that the peak of a spike could have

Lower threshold - the maximum value of voltage that the peak of a spike could have

A valid spike was saved as a waveform when it satisfied the following three criteria. A valid spike must have had its upper peak preceding the lower peak, the lower peak occurred within 0.56 ms after the upper peak, and the upper peak did not occur within 0.6 ms after the preceding upper peak. We set up these criteria, considering the duration of an action potential (about 1ms).

Order of upper peak and lower peak – the temporal order of two peaks (Upper → lower)

Upper peak to lower peak interval - the maximum time interval between two peaks (0.56 ms)

Upper peak to upper peak interval - the minimum time interval between two peaks (0.6 ms)

When a potential met all three criteria, the time of the upper peak was taken as the onset time of an individual spike. Each waveform of an individual spike consisted of 30 data points (1.2 ms) from -12 points to +17 points as of the time of the upper peak. We saved this waveform with the timing data for further analysis.

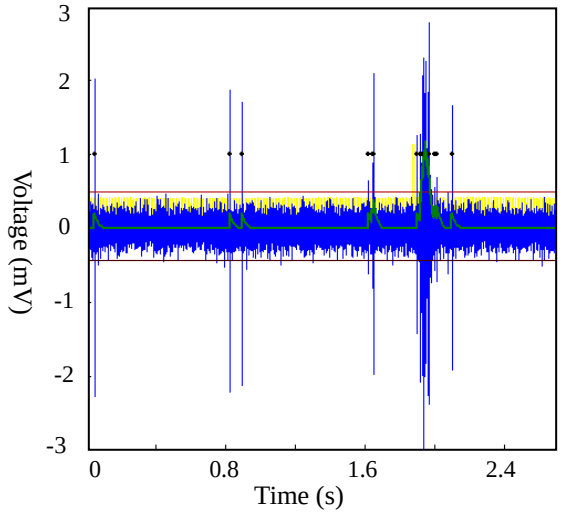

Figure 5. An example trial of spike extraction. Blue indicates extracellular potential in voltage, and the yellow is the output of photodiode. Two horizontal lines represent the upper and lower thresholds for spike extraction. Filled circles are extracted valid spikes that meet the criteria.

2.4.3. Sorting Spikes

In order to determine the number of units for each recording site, we superimposed waveforms of all valid spikes (waveforms) and typically sorted 2-4 cells with a spike sorting program which was developed in our lab using Matlab (The Mathworks, 2001). This program, called 'wavesorter', is based on principal component analysis (PCA) and k-mean clustering (Yu, 1999). First, several thousands of waveforms were randomly sampled out from all recorded waveforms, and principal components that account for as much variability in the data as possible were extracted. The number of clusters was decided by Maximum Likelihood Estimation, but the optimal cluster number (or range) was designated by the experimenter. In order to filter out spike-like potential changes that

were induced by the animal's unwanted movements or by electrical noise, we eliminated waveforms using a pruning algorithm. In this, we computed the Euclidian distance of all waveforms in each cluster from the centroid of the cluster and removed the outliers which were beyond 2 SD (standard deviation) from the centroid. We further refined sorting by selecting remaining noise spikes by visual inspection and defined as invalid-spikes, when necessary. The number of clusters extracted from the PCA was the number of cells from each recording site. After determining the centroid of each cluster, all recorded waveforms were distributed to the optimal cluster, considering Euclidian distances between each centroid and waveforms.

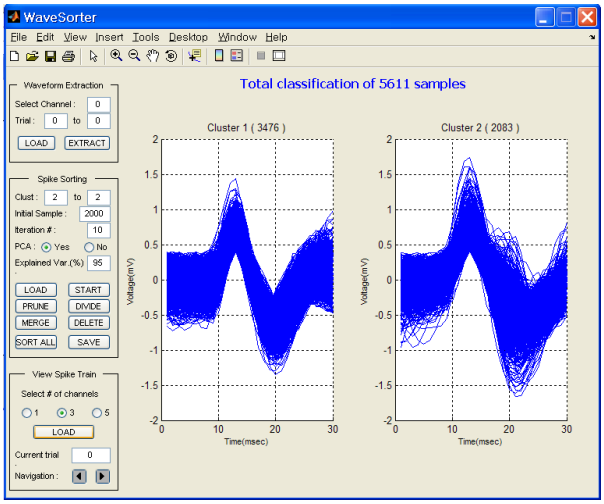

Figure 6. Two clusters extracted by the principal component analysis (#20120614).

2.4.4. Confirming the single-unit classification

As explained above, single-units were isolated on the basis of PCA (Lewicki, 1998), and discriminated on the basis of waveform shape. However, for validating the clustering by PCA, we computed inter-spike intervals for all waveforms of each single-unit. Clusters with less than 3% of inter-spike intervals of 1ms (refractory period) or less were regarded as a single-unit. Even though a cluster was isolated by PCA or had a shape significantly different from other clusters, if it had over 3% of inter-spike intervals of 1ms or less, we regarded it as a multi-unit and summed up all spikes from all clusters for further analysis.

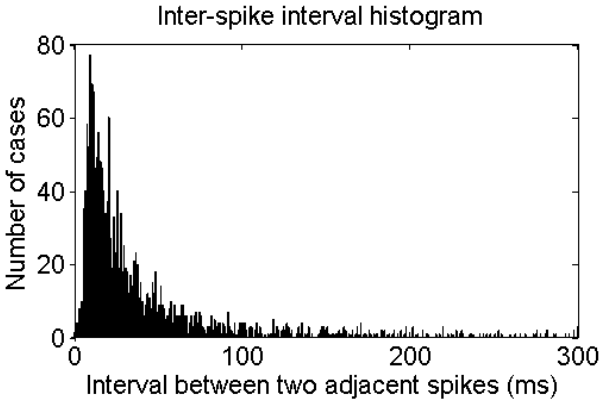

Figure 7. Example of inter-spike interval histogram (#20120822-SUA, cluster 3). Inter-spike interval of this example neuron shows clear refractory period, also less than 1% of inter-spike intervals of 1ms or less.

2.4.5. Spike density function

The timing of each spike, taken as the time of upper peak, was transformed into a binary spike train coded with 1 for spike and 0 for no spike. In order to derive a continuous index of neural activity, spike density function was calculated by convoluting the binary spike train with a growth-decay exponential function (5). This asymmetric growth-decay exponential function was known as a resemblance of postsynaptic potentials, and more accurate when it comes to latency of neural activity than a symmetric Gaussian function (Thompson et al., 1996).

$$\mathbf{RV\ (t) = (1-exp(-t/\tau_g))\ x\ (exp(-t/\tau_d))\ x\ k\ -} \quad (5)$$

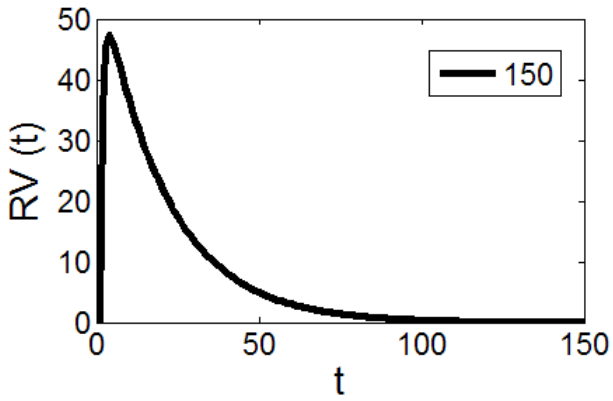

Figure 8. Growth-decay exponential function. A type of kernel function for computing spike density function. The rate (RV) plotted against time (t). The shape of the function was determined by two time constants, τ_g and τ_d. These constants represent the rate of growth and decay (in the current study, τ_g = 1ms, τ_d = 20ms). The width of function (t) was 150ms, and k was 57.8611. The originally devised growth-decay exponential function was $R(t) = [1-exp(-t/\tau_g)]x[exp(-t/\tau_d)]$ (Thompson et al., 1996).

2.4.6. Eliminating outliers

2.4.6.1. Stimulus-evoked activity level

After eliminating trials in which the eye position was unstable during fixation period (> 50 deg/s, during 50-150ms and 50-850ms after the onset of RF stimulus, each for sequence and drifting conditions), we also eliminated trials wherein the neural activity was over two standard deviations from the mean activity for each experimental condition. The standard deviation and mean value of neural activity were calculated from the duration of +50~150ms after the RF target onset (in the case of 'Sequence conditions', and +50~850ms for 'Drifting conditions' as explained below).

2.4.6.2. Mean eye position during stimulus presentation

In the current study, we compared the magnitude of neural activity evoked in response to two stimulus directions. For this comparison, we examined whether the eye position was maintained same between two stimuli conditions, because a slightly different eye position between two conditions, if any, can make a significantly different neural response to Gabor stimulus due to the change of receptive field position, and this will invalidate our comparison. Even though the eye position was always maintained within the electronically defined fixation window (typically, < 2.0 degrees in diameter) centered about fixation point, it occasionally broke the window. We first eliminated the trials deviated more than 2SDs from the mean values (Figure 9).

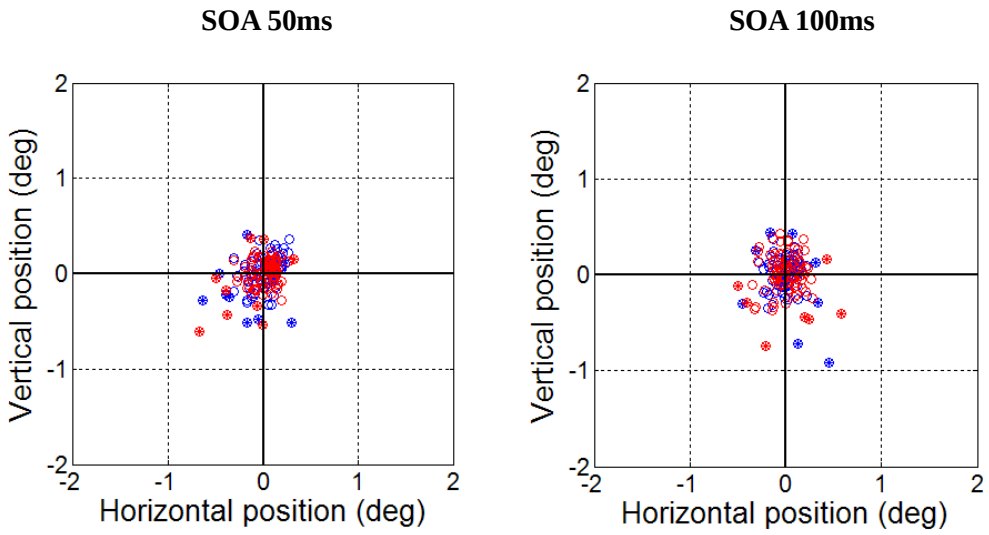

Figure 9. Determining eye position outliers with the criterion of two standard deviation (#20120730-SUA, cluster 3). Star-filled Circles indicate the eye position outliers. **Left:** horizontal and vertical eye positions for trials with the SOA of 50ms. Red circles are sequential condition 1 and blue circles are sequential condition 2. **Right:** eye positions for trials with the SOA of 100ms.

We analyzed horizontal and vertical eye positions during the duration of stimulus presentation (sequential condition: 20ms, drifting condition: 800ms). There were four sessions wherein the mean eye positions were significantly different between two directions of sequential conditions, and these were eliminated from further analysis.

SOA 50ms

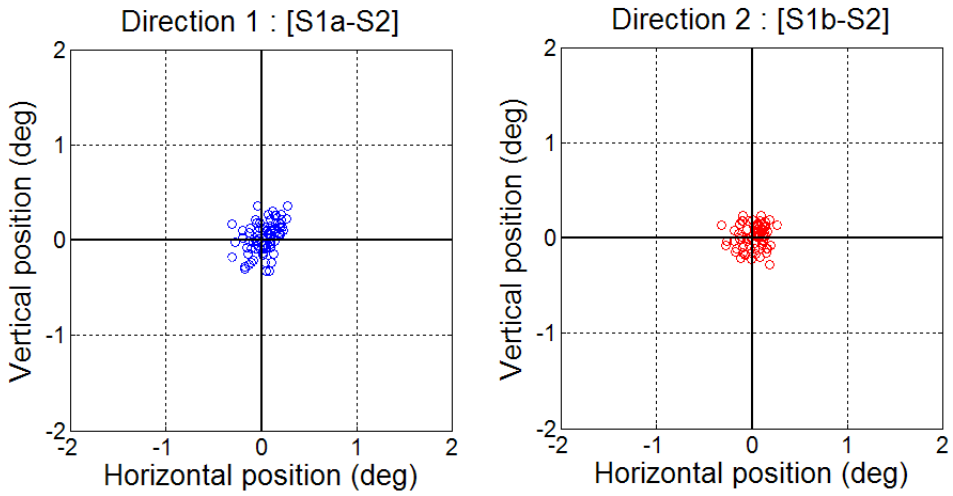

Figure 10. Eye position between two directions after deleting outliers of Figure 9 (#20120730-SUA, cluster 3). Left: horizontal and vertical eye positions for [S1a-S2] condition in SOA of 50ms. **Right:** horizontal and vertical eye positions for [S1b-S2] condition in SOA of 50ms.

2.4.6.3. Non-reactivity of surround

Many studies dealing with surround interaction typically used an annulus as a surround stimulus to drive maximal surround modulation effect (Cavanaugh et al., 2002). However, we used peripheral Gabor patches (S1a, S1b) placed 1.5 cRF diameters away from the RF for deriving a global direction of apparent motion by using two sequential Gabor stimuli. In the current study, we distinguish the directional selectivity between stimulus motion confined within the RF ('local directionality') and motion extending outside the RF ('global directionality'). For this, it was critical to control whether the stimulus was or was not confined within the RF. For measuring global directionality, preceding stimulus (S1) should always be located in the surround region of the RF, yet following stimulus

(S2) should be located inside the RF. We tested this by presenting the S1 or S2 alone outside the receptive field, and whether these evoke any spike response. Three control conditions were added to the main experiment, the same target with the duration of 20ms in different spatial position, S2 (cRF), S1a and S1b.

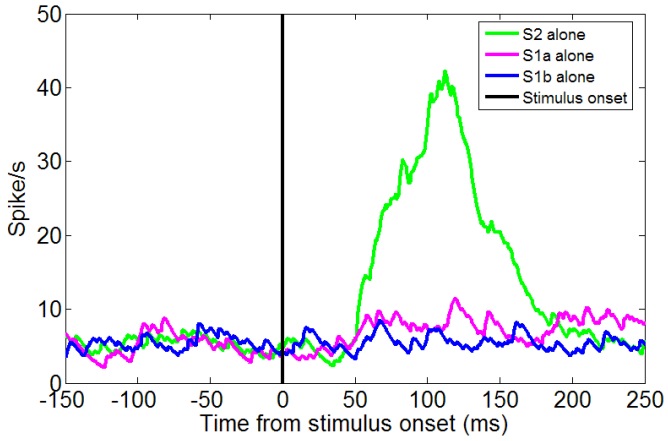

Figure 11. Example spike density plot showing surround reactivity (#20120705-SUA, cluster 3). This unit was regarded as an invalid unit since we established a criterion that the S1 alone (S1a or S1b) should not elicit spiking responses above 5% of responses to the S2 alone.

In the example of Figure 11, even though the response during the post-stimulus time period of 50-150ms after RF stimulus (S2) onset was much greater (22 spikes/s), the same stimulus at surround regions (S1a, S1b) evoked a weak neural activities (S1a: 2.4 spikes/s, S1b: -0.02 spikes/s). We eliminated this unit from SUA dataset, because the response to the surround target 'S1a' was larger than 5% of the RF responses (5% of S2-alone response was about 1.1).

Summary of steps for obtaining finalized dataset

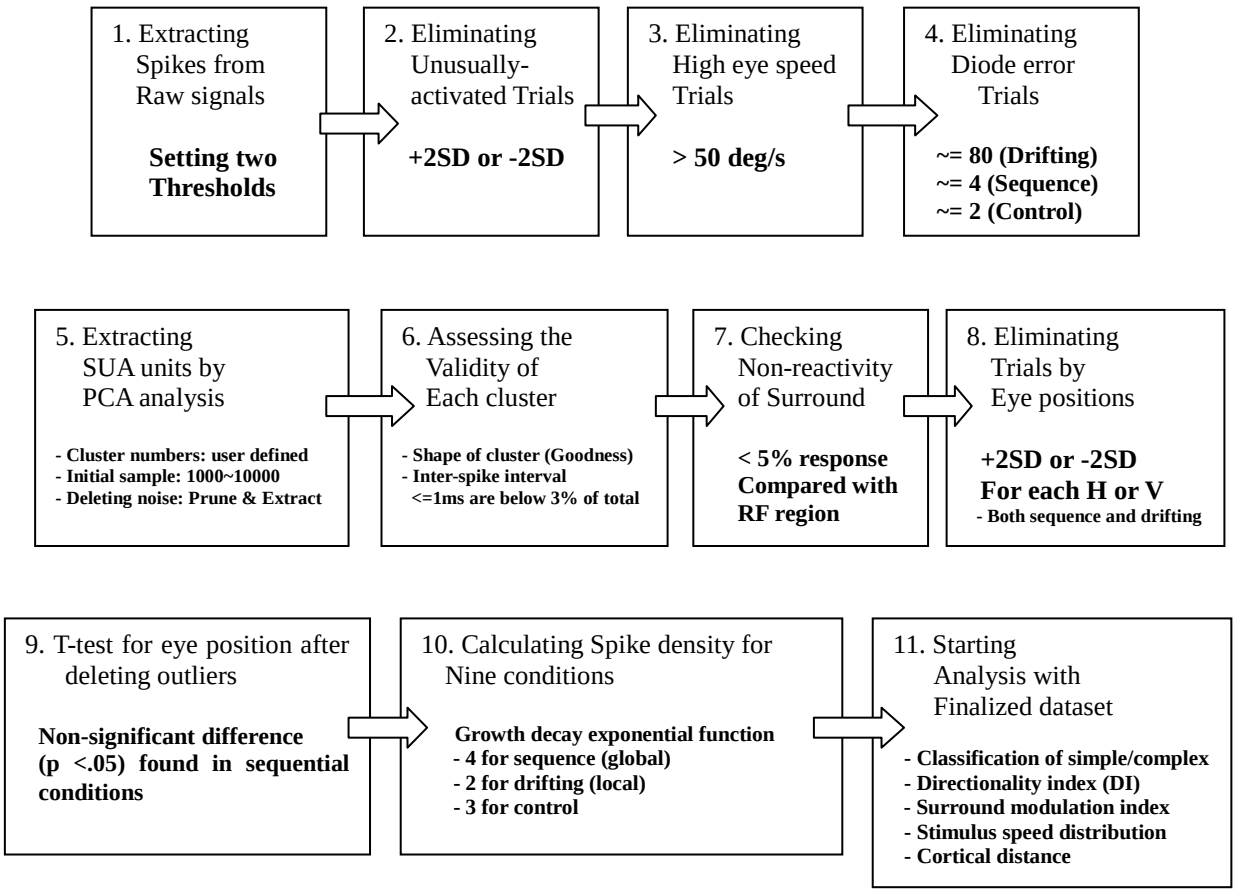

2.5. Methods of data analysis

2.5.1. Direction selectivity

The direction selectivity (or 'directionality') is a basic property of motion-sensitive neurons, and thus the properties of direction selective neurons in V1 have been intensively studied. Classically, direction selectivity was computed as a **'Direction selectivity index (DI)'**, which is typically defined as the difference in mean spike response between preferred and non-preferred direction, and proportioned by dividing the mean spike response of preferred direction (often expressed as Eq.6, Gur et al., 2007). If the value of DI is 0, it represents that the neurons do not have any preference for motion direction, and two opposite motion directions evoke the same level of responses. If the value of DI is 1, it indicates that the neuron responds to only one direction. Neurons of DI >0.5 are commonly regarded as direction selective. We calculated local DI with Eq. 6 as mentioned above. For global DI, we used two equations 7 and 8 depending on consistency with local DI. In the formula, NP refers to the mean spiking response evoked by non-preferred direction, whereas P refers to the mean spiking response evoked by preferred direction.

$$\textbf{Local DI} = 1 - NP/P \quad - \quad (6)$$

$$\textbf{Global DI} = 1 - NP/P \quad \textbf{or} \quad \textbf{Global DI} = -(1 - NP/P) \quad - \quad (7), (8)$$

The local DI ranged from 0 to 1. Yet, the global DI ranged from -1 to 1, depending on whether the directional preference matched with local DI or not. If a neuron had the same preference of direction in local and global (ex. leftward: +90 degree), the global DI value was positive. In the opposite case, we put a negative sign to global DI. The analysis

window for calculating global DI ranged from 50 to 150ms after the onset of S2 stimulus, and for local DI, from 50 to 800ms. However, for local DI of simple cell, we used the ratio of amplitudes of F1 component and the analysis duration differed depending on their temporal frequency and the characteristics of response time course.

Another way to compute the direction selectivity index was use of both negative and positive signs for local DI, too. Regardless of whether a motion was local (drifting Gabor stimulus) or global (sequential Gabor stimuli), if a neuron preferred an upward (or left) direction of motion, a positive sign was added to the value from a formula (1-NP/P). On the contrary, if a neuron preferred a downward (or right) direction of motion, a negative sign was added to the value from a formula (1-NP/P).

$$\textbf{Local and Global\_DI}_{\textbf{up}} = \mathbf{1 - NP/P} \quad - \quad (9)$$

$$\textbf{Local and Global\_DI}_{\textbf{down}} = \mathbf{-\,(1-NP/P)} \quad - \quad (10)$$

The advantage of this method was the same formula applies equally to both local and global DIs, thus, local and global DI were defined with directions of motion in the screen. We will compare results from this method (Eq.9-10) to the previous method (Eq. 6-8) in the part [3.3.3.1].

2.6. Experiment procedures

2.6.1. Receptive field mapping

Steps for determining characteristics of receptive fields

1. Horizontal & Vertical positions (Qualitative)
2. Orientation
3. Horizontal & Vertical positions
4. Size
5. Direction (Qualitative)
6. Spatial frequency
7. Temporal frequency

The properties of V1 neuron were determined by several mapping procedures. Horizontal and vertical positions of receptive field were first estimated with a manually-controlled rotating sinusoidal grating while the monkey fixated on the central red point. After roughly defining the RF position, we typically presented flickering cosine gratings with one of five orientation candidates (0-150° in 30° intervals, 2° diameter). They were presented for 200ms and randomly repeated five times for forward correlation analysis. Mean firing rate of y-axis was obtained by averaging the number of spikes during the period 50-200ms after stimulus onset. We chose the value of parameter that produced maximal neuronal responses. Tuning curve was fitted by DoG (Difference of Gaussian, Eq.11 and 12). The initial values for these tuning curve functions are given in the text box below. Most of technical programs in this section were developed by Kim (2007).

$$DoG_1(x) = k_1 \text{ x } \exp\left(\frac{-(x-c)^2}{2\sigma_1^2}\right) - k_2 \text{ x } \exp\left(\frac{-(x-c)^2}{2\sigma_2^2}\right) + l \qquad (11)$$

$$DoG_2(x,y) = \left\{k_{x1} \text{ x } \exp\left(\frac{-(x-c_x)^2}{2\sigma_x^2}\right) - k_{x2} \text{ x } \exp\left(\frac{-(x-c_x)^2}{2\sigma_{x2}^2}\right)\right\} \text{ x } \left\{k_{y1} \text{ x } \exp\left(\frac{-(x-c_y)^2}{2\sigma_{y1}^2}\right) - k_{y2} \text{ x } \exp\left(\frac{-(x-c_y)^2}{2\sigma_{y2}^2}\right)\right\} + l \qquad (12)$$

k_1 : observed the maximum mean firing rate

c : the condition value that elicits the maximum mean firing rate

σ_1 : 1/5 of parameter range which for stimulus generating / or 1 (choose more large value)

k_2 : 1/3 of the maximum mean firing rate

σ_2 : 1/3 of parameter range which for stimulus generating / or 1 (choose more large value)

l : Mean of the mean firing rate of all conditions

More precise RF positions were determined by following quantitative methods using a smaller (typically, 1° diameter) optimally oriented stationary sinusoidal grating. The RF size was also tested with a stationary circular Gabor patch of a varying diameter. In most sessions, we determined the optimal RF diameter that elicits the largest spiking responses. Before spatial and temporal frequency preference testing, one of two drifting directions (both orthogonal to preferred orientation) that showed a larger response was qualitatively selected. Tuning curves of spatial (cycles per degree: 0.25, 0.5, 1, 2, 4, 8, 16) and temporal frequencies (cycles per second: 0.5, 1, 2, 4, 5, 10, 20) were generated by using drifting sinusoidal grating that had optimal RF properties. Throughout all mapping procedures, the contrast of stimulus was 100%. In most main experiments, the contrast of stimulus was 64% (32% for two recording sessions, Table 3).

2.6.2. Main experiment

We recorded spike activity of V1 neurons while each of two male macaque monkeys performed a simple fixation task. Trials of six experimental conditions were randomized within a block. To measure local directionality, we tested two stimulus conditions in which a Gabor stimulus drifted for 800ms in two opposite directions orthogonal to optimal orientation (Figure 12). To measure global directionality, we tested four stimulus conditions for two directions of stimulus sequence, S1 and S2, each for 20ms (Figure 13). We targeted to measure two types of directionality and tried to find the relationship between them.

Drifting stimulus condition

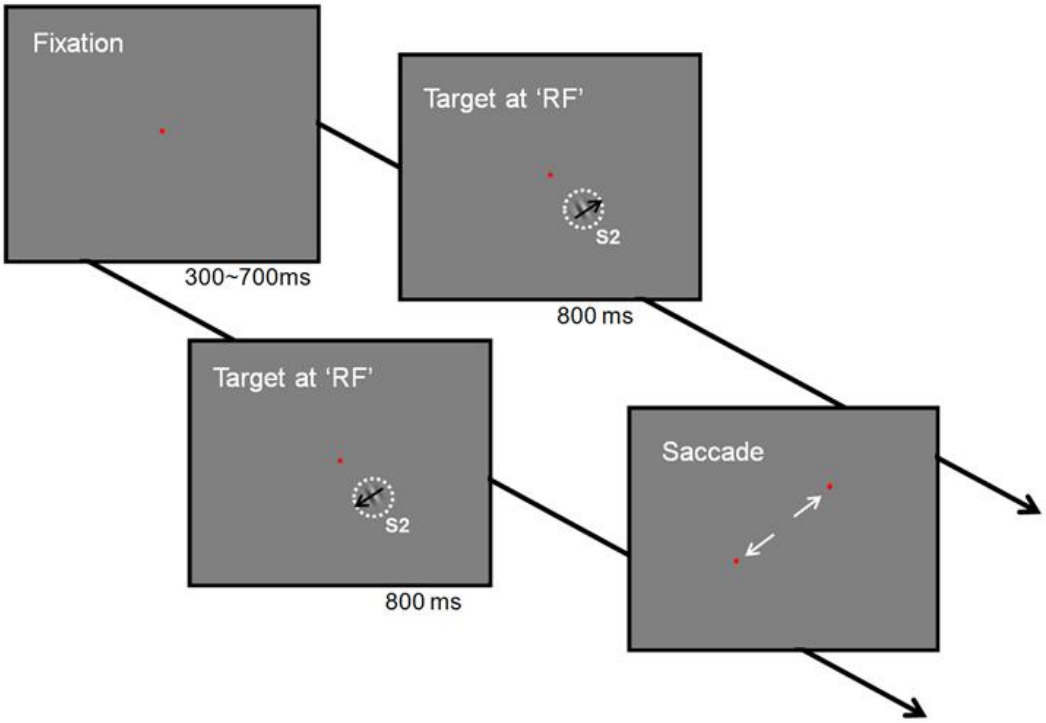

Figure 12. Measuring local directionality. Local directionality was quantified with mean spike densities for two local drifting directions confined within the cRF. If a cell was classified as a simple cell based on F1/F0 ratio, its local directionality was instead quantified with the ratio of F1 (the amplitude of the first harmonic response matching to the temporal frequency of the drifting Gabor). Saccade target was presented at one of two positions, +3.5 (H) and −3.5 (V) or −3.5(H) and −3.5 (V).

Sequential stimulus condition

Figure 13. Measuring global directionality. Global directionality was quantified with mean spike densities for the two sequence directions. Sequential stationary Gabor stimuli of 20ms each with SOA of 50 or 100ms; S1 was presented 1.5 cRF diameters away from the center of cRF at either side along sequence direction that was orthogonal to preferred orientation, and S2 was presented within the cRF. Saccade target was presented at one of two positions, +3.5 (H) and −3.5 (V) or −3.5(H) and −3.5 (V).

3. Result

3.1. Data summary

Subject	# Session (site)	Single-unit (A)	Multi-unit (B)	Total (A+B)
DC	27	29	7	36
IR	19	22	4	26
Total	46	51	11	62

Table 2. Data summary of two subjects

We analyzed spiking activities of 51 single and 11 multi-units from 46 recording sessions. Data from another eight recording sessions were discarded, since in those sessions, we failed to isolate spatially distinctive cRF from the eCRF (extra-classical receptive field) or found a statistically significant difference (t-test, <.05) in eye position (horizontal or vertical) between sequential conditions after deleting eye position outliers. Although we tried to isolate single-unit for each recording session, it was not always possible. Each single-unit was isolated by waveform shape and inter-spike interval (see, 'Method'). Finally, 51 single-units were isolated from 35 recording sessions, and 11 multi-units from another 11 recording sessions. Parameters and measured values of all valid units are summarized in Table 3.

#	Date	Dia	Pos.H	Pos.V	Orien	Contrast	SF	TF	Local DI	Global DI (50)	Global DI (100)
1	120614	1.6	2.7	-2.94	150	64%	1	4	0.455	0.256	-0.262
2	120614	1.6	2.7	-2.94	150	64%	1	4	0.294	**0.447***	0.1
3	120618	1.6	2.7	-2.9	60	64%	1	0.5	0.507	**0.262***	0.113
4	120627	1.5	2.9	-3.2	60	64%	1	1	0.173	0.165	**0.214***
5	120703	1.8	3	-2.4	60	64%	4	0.5	0.053	**0.12***	**0.11***
6	120705	1.8	3.3	-2.9	90	64%	4	4	0.213	**-0.29***	**-0.130***
7	120709	1.9	3.5	-2.7	90	64%	2	0.5	0.097	-0.064	**-0.076***
8	120711	1.8	3.4	-2.68	90	64%	16	0.5	0.077	0.126	**-0.487***
9	120718	1.6	3.1	-3.1	150	64%	4	5	0.104	**-0.235***	**-0.106***
10	120719	1.6	3.2	-3.6	120	64%	2	1	0.006	0.056	-0.044
11	120725	2	3	-3.1	90	64%	4	1	0.160	**0.298***	**0.121***
12	120725	2	3	-3.1	90	64%	4	1	0.105	**0.181***	-0.087
13	120807	1.6	3	-2.7	30	64%	1	4	0.383	0.313	-0.473
14	120730	1.6	3.2	-3	50	64%	2	1	0.013	-0.071	**0.244***
15	120730	1.6	3.2	-3	50	64%	2	1	0.307	**-0.115***	**0.018***
16	120816	1.4	3.6	-3	160	64%	2	10	0.051	**-0.042***	**-0.018***
17	120820	1.6	3.4	-2.7	170	64%	4	0.5	0.157	0.007	**0.203***
18	120822	1.8	3.5	-2.8	90	64%	4	4	0.076	**-0.155***	**-0.133***
19	120822	1.8	3.5	-2.8	90	64%	4	4	0.026	-0.085	**0.2***
20	120822	1.8	3.5	-2.8	90	64%	4	4	0.2501	**-0.054***	**0.115***
21	120829	1.6	3.8	-2.9	100	64%	8	0.5	0.042	-0.145	-0.011
22	120830	1.6	3.3	-2.9	60	64%	2	2	0.266	**0.219***	-0.138
23	120903	1.6	3.2	-2.8	60	64%	4	0.5	0.172	**0.032***	-0.133
24	120905	1.5	3.39	-3.2	0	64%	2	4	0.003	0.049	-0.003
25	120912	1.5	3.6	-2.8	80	64%	16	2	0.071	**0.325***	**0.017***
26	120913	1.8	3.6	-2.9	30	64%	4	5	0.029	-0.015	**0.057***
27	120917	1.6	3.5	-3.1	0	64%	4	5	0.059	**0.168***	**-0.092***
28	120917	1.6	3.5	-3.1	0	64%	4	5	0.021	**-0.078***	**-0.007***
29	120920	1.2	3.8	-2.9	0	64%	4	4	0.151	-0.07	**0.171***

30	121107	1.6	-2.6	-2.4	150	64%	4	4	0.072	**-0.367***	**0.128***
31	121107	1.6	-2.6	-2.4	150	64%	4	4	0.119	-0.075	**-0.453***
32	121108	2.2	-2.6	-2.21	60	64%	2	5	0.184	-0.124	**-0.098***
33	121108	2.2	-2.6	-2.21	60	64%	2	5	0.462	0.367	**-0.119***
34	121114	2.2	-2.1	-2.3	20	32%	4	4	0.039	**-0.054***	-0.053
35	121115	2.2	-2.4	-2.3	0	32%	4	5	0.180	**-0.163***	-0.064
36	121115	2.2	-2.4	-2.3	0	32%	4	5	0.214	0.044	**0.131***
37	130104	1.2	2.1	-0.6	105	64%	2	0.5	0.221	-0.053	**0.125***
38	130104	1.2	2.1	-0.6	105	64%	2	0.5	0.049	0.237	-0.078
39	130117	1.8	-4.6	-2.6	120	64%	2	5	0.058	-0.245	0.432
40	130205	1.5	-4.26	-3.46	120	64%	1	5	0.122	**0.012***	-0.099
41	130206	1	-4.5	-3.6	0	64%	4	1	0.059	-0.131	0.339
42	130206	1	-4.5	-3.6	0	64%	4	1	0.077	**-0.59***	-0.066
43	130214	2.2	-5.7	-3	90	64%	1	4	0.033	0.088	**-0.064***
44	130220	2.2	-6.3	-2.2	15	64%	1	2	0.060	**0.151***	**-0.091***
45	130220	2.2	-6.3	-2.2	15	64%	1	2	0.041	0.041	0.009
46	130226	1.4	-5.3	-2.6	90	64%	4	5	0.18	0.2	**0.301***
47	130226	1.4	-5.3	-2.6	90	64%	4	5	0.138	**-0.541***	**0.615***
48	130307	2.2	2.17	-0.61	60	64%	1	10	0.16	-0.019	**-0.419***
49	130308	1.6	2	-0.8	0	64%	16	0.5	0.128	**0.201***	**0.135***
50	130405	1.6	2.2	-1.3	150	64%	2	2	0.116	0.117	-0.189
51	130510	2	2.57	1.98	150	64%	8	4	0.115	**0.405***	**-0.581***
52	130523	1.4	2.7	2.3	30	64%	2	20	0.216	0.457	**-0.612***
53	130527	1.8	3.5	1.7	120	64%	1	5	0.186	-0.302	**-0.035***
54	130604	2	2.8	1.9	0	64%	2	2	0.065	**-0.124***	**-0.085***
55	130604	2	2.8	1.9	0	64%	2	2	0.066	**-0.1***	-0.056
56	130611	3.2	2.4	2.4	90	64%	2	0.5	0.127	**0.287***	0.107
57	130624	2	2.2	2.7	90	64%	1	5	0.452	**-0.177***	0.051
58	130624	2	2.3	2.7	90	64%	1	5	0.602	**0.652***	0.231
59	130625	3.8	2.48	2.04	0	64%	4	0.5	0.058	**-0.208***	-0.285*

60	130702	2.6	2.8	2.4	0	64%	2	1	0.156	0.251	**0.101***
61	130702	2.6	2.8	2.4	0	64%	2	1	0.193	-0.012	**-0.106***
62	130708	2.6	3.3	2	0	64%	2	1	0.006	**-0.058***	**0.064***

Table 3. Parameters and measured values of all valid units. First and second column of this table indicate the number of unit and the date of recording session, respectively. After RF mapping procedures, diameter (deg), positions (deg, horizontal and vertical), orientation (deg), spatial (cycles/deg) and temporal frequency (cycles/s) of RF were set as optimal values. The last three columns shows measured local and global directionality indexes. Among all global directionality indexes (N=62) for SOA of 50ms, 32 units (51%) were classified as a unit with significant difference in more than 1ms between opposite directions (t-test, $p<.05$). In SOA of 100ms, 39 units (62%) showed significant difference between opposite directions (t-test, $p<.05$). Significant units were asterisked (*). T-test was done with the duration of 50-150ms after the onset of S2 stimulus. These local and global directionality values were calculated with Eq. 6-8.

3.2. Classification of simple and complex cell

3.2.1. Criterion of Simple and complex cells

Simple/complex cells were determined by the criterion of F1/F0 ratio (Skottun et al., 1991; Henry et al., 2013). This ratio shows the relative response modulation to drifting sinusoidal grating at a preferred temporal frequency (testing range: 0.5 to 20 Hz). F0 was obtained from calculation of the mean firing rate for duration of drifting stimulus presentation. F1 was taken from the amplitude of the first harmonic response matching to the temporal frequency of the drifting sinusoidal grating or Gabor. Most of recorded cells showed a tendency toward very low F1/F0 ratio (mean < 0.3 in Figure 14-A, mean < 0.4 in Figure 14-B).

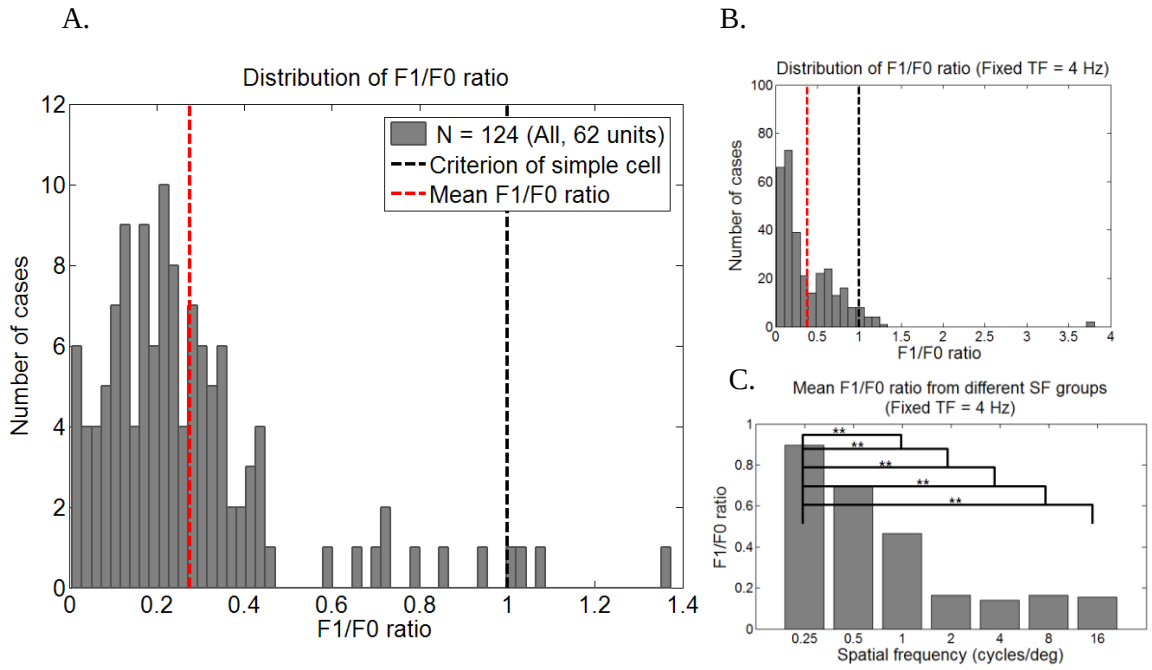

Figure 14. Distribution of F1/F0 ratio. A. Distribution of F1/F0 ratio of overall recording units for two drifting conditions (N=124). Based on

the classical criterion of simple/complex cell, 58 of 62 recorded cell defined as a complex cell. We did not classify each cell as a simple/complex in mapping stage. This figure is based on spiking responses to two drifting Gabor stimuli in the main experiment. **B.** Distribution of F1/F0 ratio of spatial frequency (SF) mapping sessions, with fixed 4Hz temporal frequency (315 cases from 45 sessions). **C.** Mean F1/F0 ratio of seven different SF groups (0.25, 0.5, 1, 2, 4, 8, 16). Statistically significant mean differences found between different SF groups (t-test, $p<.01$).

Figure 15 illustrates the estimation of amplitude of response modulation using by sum of sine wave fitting provided by 'cftool' in Matlab. The mean spike responses are expressed as dots as a function of time. These dots are well-fitted by sine wave function, producing the value of a1 (amplitude).

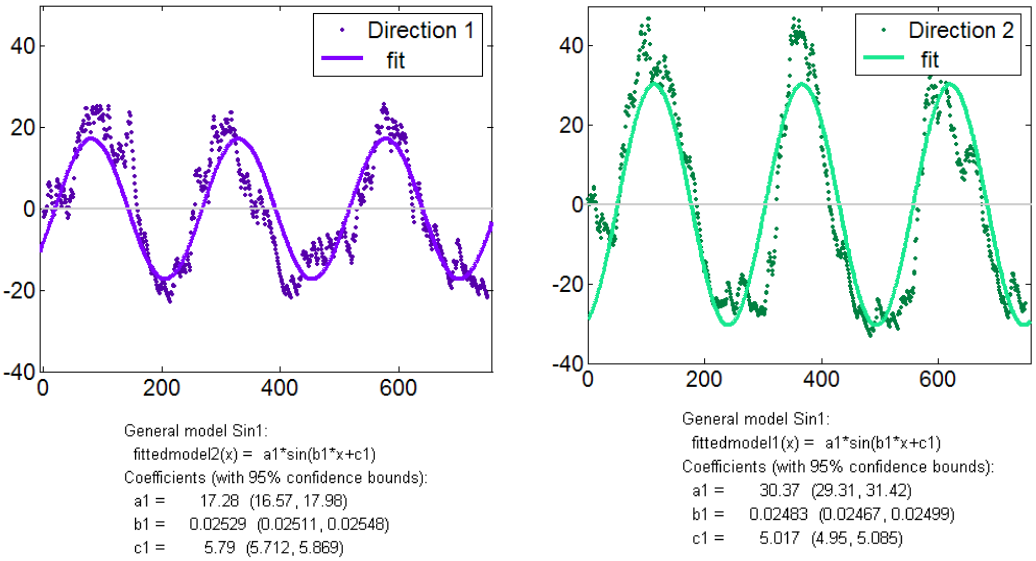

Figure 15. Sine-wave fitting for measuring response modulation to 4Hz temporal frequency (#20120614-SUA, cluster 1). The amplitude of response modulation was 17 spikes/s for the direction 1, yet 30 spikes/s for the direction 2. Therefore, the local DI was 0.43, which was computed by a formula (1-NP/P).

The result (a1 = the amplitude of neural response matching to stimulus frequency) in Figure 15 was very similar to the result of the Fourier analysis. We calculated the amplitude of the first harmonic response by using the 'fft' function in Matlab, and obtained values of 17.2 for Direction 1 and 31.6 for Direction 2. Thus, the local DI was 0.45 that was similar to the local DI from Sine-wave fitting (local DI = 0.43, Figure 15). In the case of Figure 15, the analysis window used for both methods (Sine-wave fitting & Fourier analysis) was 150 ~ 900ms after the onset of stimulus, since the onset time of the stimulus phase-locked response delayed by about 150ms.

3.2.2. Response pattern to different spatial and temporal frequencies

3.2.2.1. Response pattern depending on various spatial frequencies

During the receptive field mapping procedures, interesting aspects were found from spatial frequency mapping. As can be seen in Figure 16, spiking responses well followed the temporal frequency (TF) of drifting stimulus until 1 cycle/deg. Middle (2 and 4) and high (8 and 16) spatial frequencies (SF) did not make response modulation that locked to the stimulus temporal frequency (TF = 4Hz, fixed in spatial frequency mapping). These aspects were well displayed in Figure 14-C.

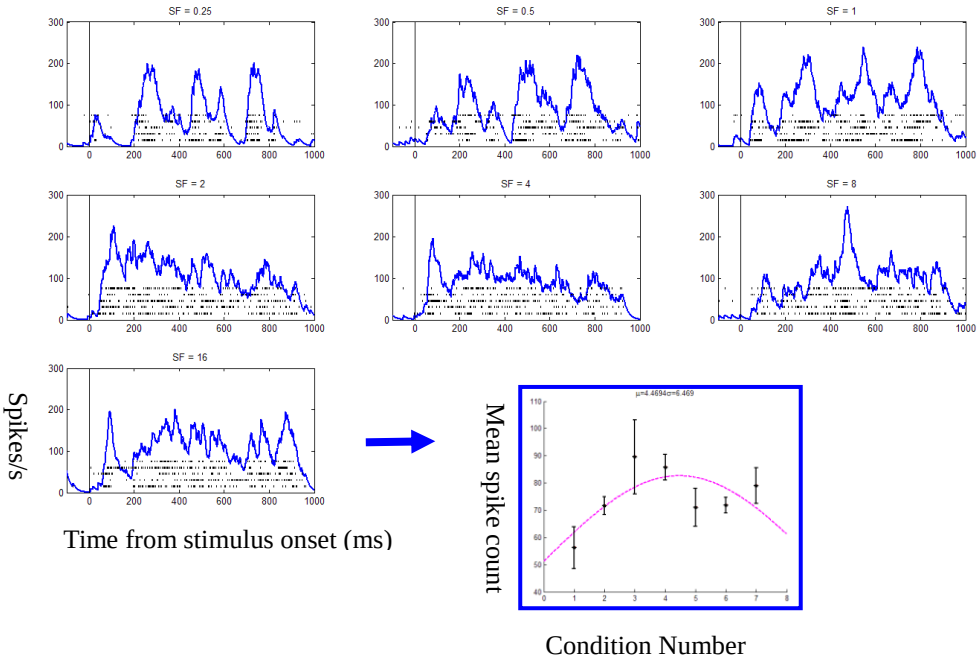

Figure 16. Example of different response patterns depending on different spatial frequencies (SF). The speed (Hz) was always 4Hz for spatial frequency mapping. Seven different spatial frequencies (0.25 / 0.5 / 1 / 2 / 4 / 8 / 16) were used for determining an optimal spatial frequency. We selected the value which elicited maximum spike counts that was 1 cycle/deg, without considering the amplitude of F1 component. The last graph indicates the tuning function (#20120614-SUA).

3.2.2.2. Response pattern depending on various temporal frequencies

Even though we selected the optimal spatial frequency (1 cycle/deg, Figure 16), while the temporal frequency mapping, there were weaker responses than during spatial frequency mapping (Figure 17). Yet, there was still strong and stimulus phase-locked responses with TF=4. Therefore, we determined an optimal temporal frequency as 4Hz which elicited maximum spike counts.

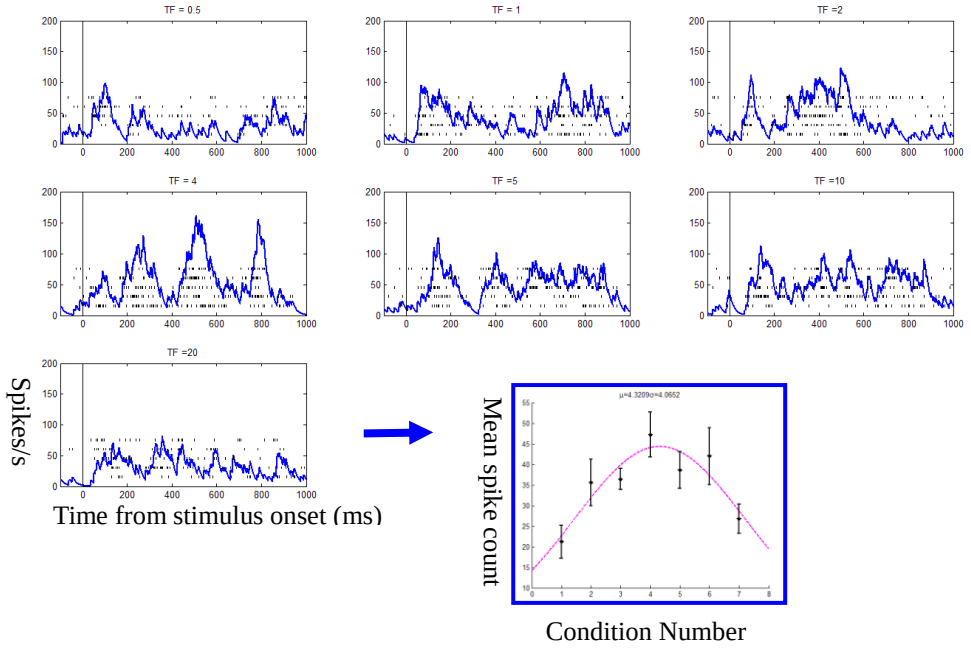

Figure 17. Example of different response patterns depending on different temporal frequencies (TF). The spatial frequency (cycle/deg) was 1Hz. Seven different temporal frequencies (0.5 / 1 / 2 / 4 / 5 / 10 / 20) were used for determining an optimal temporal frequency. We selected the value that elicited maximum spike counts, that was 4 Hz, without considering the amplitude of F1 component. The last graph indicates the tuning function (#20120614-SUA).

3.3. Local and global directionalities

3.3.1. Representative cell implying positive relationship

For some neurons, a significant positive correlation was found between local and global directionalities, indicating that V1 neurons tend to prefer the global motion direction that matched with their local directional preference. Figure 18 illustrates the spatial layout and information of cRF of one example neuron.

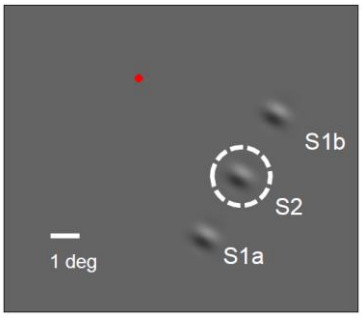

Receptive field information (S2)

- Position : +2.7 deg (H), -2.9 deg (V)
- Orientation : 150 deg
- cRF diameter : 1.6 deg
- Spatial frequency : 1 cycle/deg
- Contrast : 64%

Figure 18. Spatial layout and receptive field information (#20120614, a simple cell).

This neuron preferred a Gabor stimulus in orientation tilted at an angle of 150 degrees at a position of +2.7 (horizontal) and -2.9 (vertical) degrees. In sequential conditions, S1 was presented 1.5 cRF diameters away from the center of cRF (S2) at either side along sequence direction that was orthogonal to preferred orientation, and S2 was presented within the cRF.

Figure 19 shows raster plots of 'alone' conditions (control conditions), sequential conditions and drifting conditions (experimental conditions). Although S1 alone did not

make spiking responses, S1-S2 sequence revealed a directional preference. In the raster of sequential conditions, the first black line indicates the onset time of S1 stimulus, the second black line indicates the onset time of S2 stimulus.

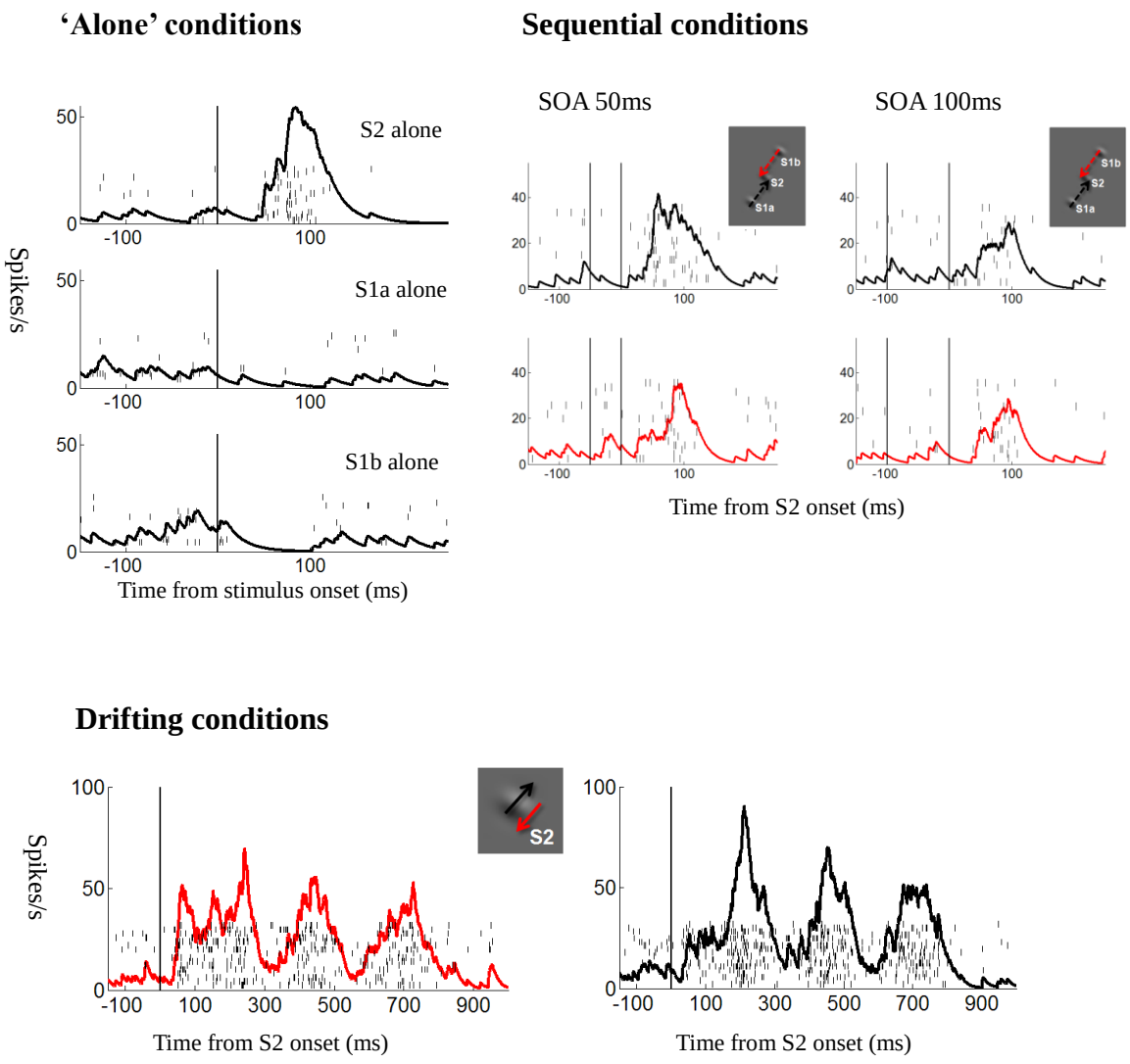

Figure 19. Raster plot of an example cell (#20120614-SUA, cluster 2).

To compare the activity more directly, we calculated the spike density function by convoluting the spike train with a growth-decay kernel function (Eq.5). And we compared each activity to another according to their experimental conditions (Figure 20).

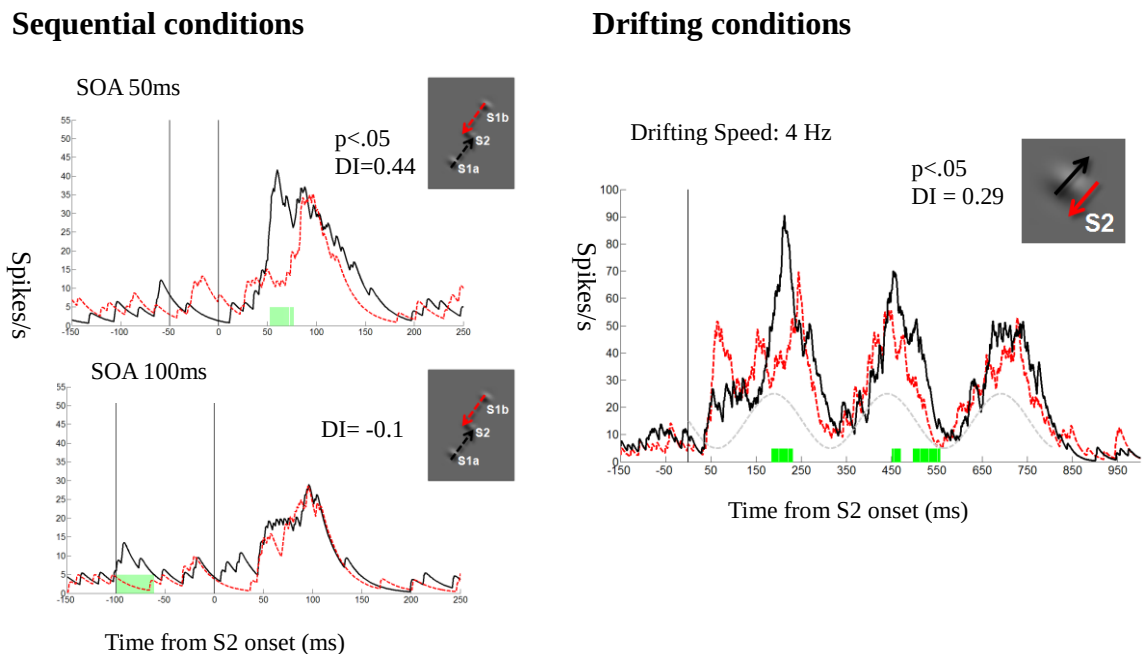

Figure 20. Comparing spike densities with t-test (#20120614-SUA, cluster 2). In this figure, DIs (direction selectivity index) were calculated with Eq.6-8, thus the DI of sequential conditions ranged from -1 to +1, yet the DI of drifting conditions ranged from 0 to +1.

Figure 20 illustrates that the S1 presented at either side of the cRF did not evoke spiking responses (see, the interval between two black lines), but the different position of the S1 evoked different cell activities. In the SOA of 50ms, this difference is more evident than in the SOA of 100ms (t-test, p<.05). In the sequential conditions, we calculated the direction selectivity by comparing mean spike densities of two different S1 conditions

(global DI for SOA50 = 0.44, for SOA100 = -0.1). Clearly, the response to the S2 was significantly modulated by the position of the S1 with the SOA of 50ms. It is noteworthy that the impression of S1b 'alone' in Figure 19 partly predicts the result of sequential condition for SOA of 50ms in Figure 20, the suppressive effect of S1b target exerted its effect on the early part of responses to S2 target. In the drifting conditions, since this was a simple cell (F1/F0 = 1.01), spiking responses followed the temporal frequency of stimulus (4Hz) very well. Gray dashed line shows the stimulus temporal phase. Green bars indicate the duration of significant difference between two S2 directions (t-test, $p<.05$). After calculating the amplitude of F1 component of two drifting conditions, we compared these two amplitudes and quantified the direction selectivity (local DI = 0.29).

Figure 21 shows the results from another neuron from the same recording day (#20120614-SUA, cluster 1). In general impression, the raster and comparison plot of this neuron were similar to the previous neuron (#20120614-SUA, cluster 2). The suppressive effect of S1b target also exerted its effect on the early part of responses to S2 target as Figure 20 (SOA 50ms, in Figure 21).

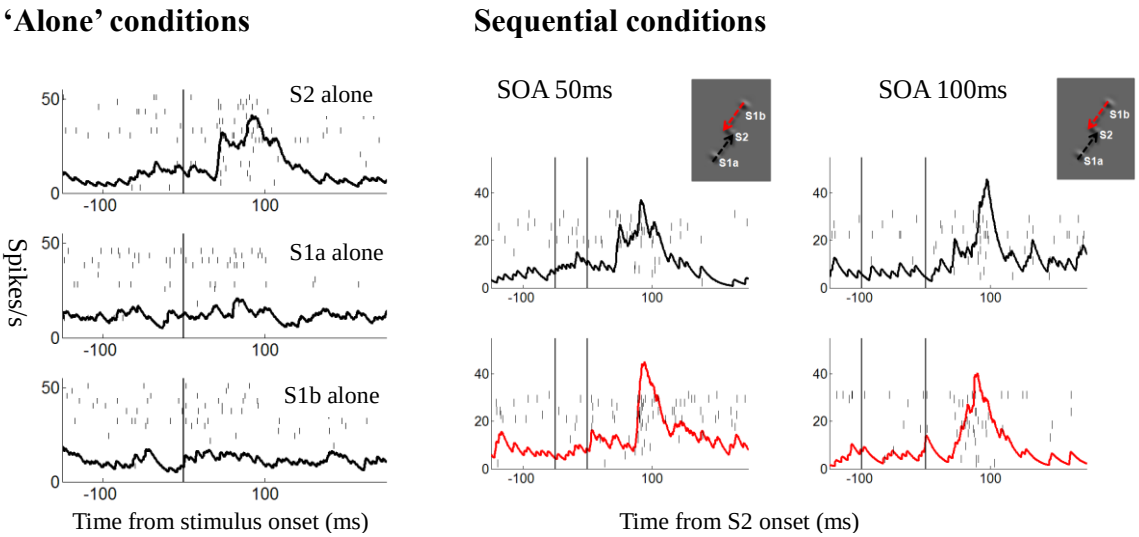

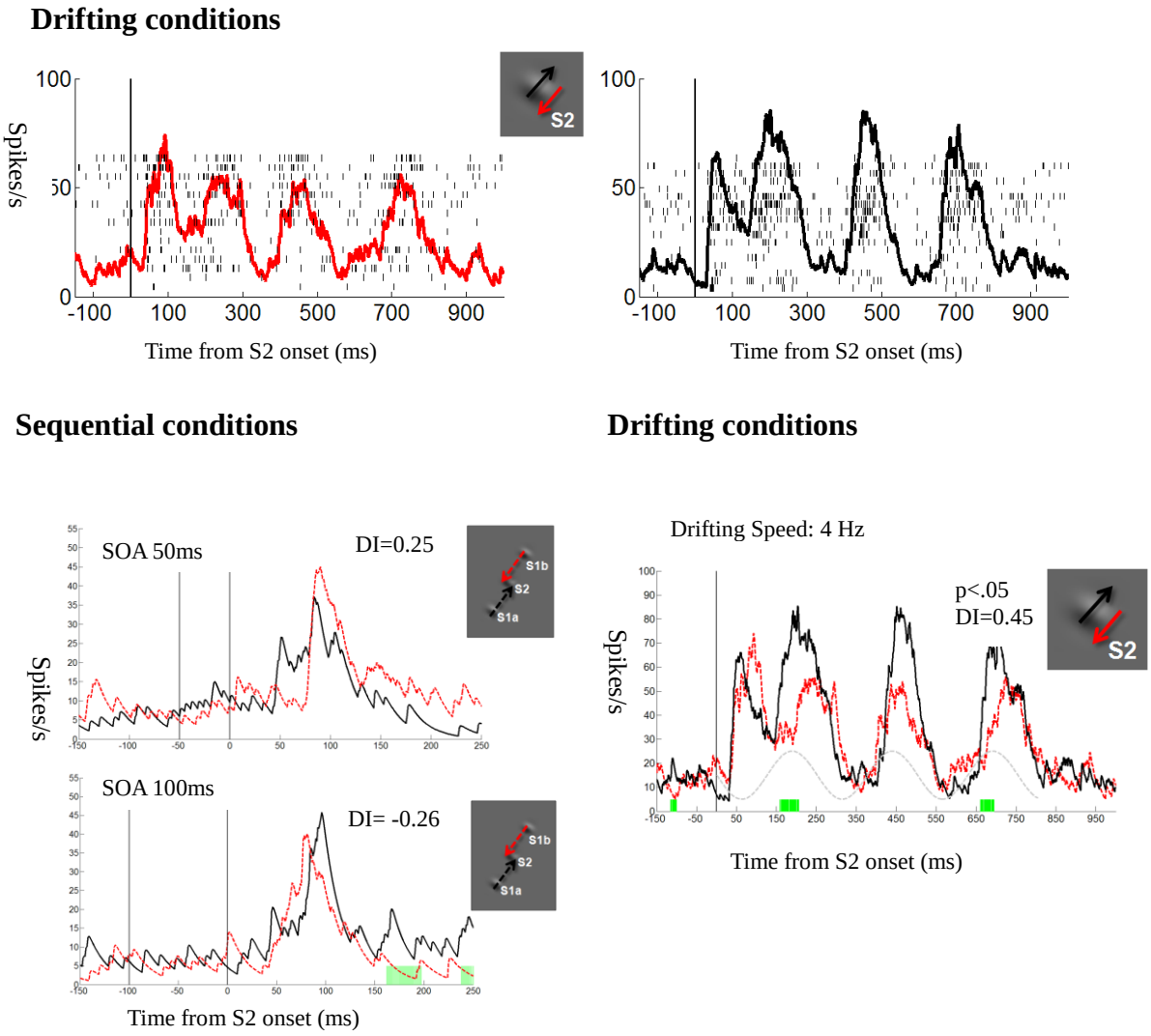

Figure 21. Raster and comparison plot of an example cell (#20120614-SUA, cluster 1). DIs (direction selectivity index) were calculated with Eq.6-8, thus the DI of sequential conditions ranged from -1 to +1, yet the DI of drifting conditions ranged from 0 to +1.

3.3.2. Representative cell showing the effect of surround is differed by the SOAs

According to previous study (Kim et al., 2012), the modulation by surround interaction is highly sensitive to small changes in spatiotemporal aspects of cRF surround. The neuron reviewed in [3.3.1.] was sensitive to the position of surround target, and it was also selective to different SOAs. Here, results from another representative cell (#20130510) depicted this characteristic quite well. Global DI became negative values when sequential conditions with SOA of 100ms (Figure 23). The neuron was highly sensitive to the temporal interval of sequential stimuli. Even the 50ms change of SOA made the preference for global direction opposite (0.4 → - 0.58).

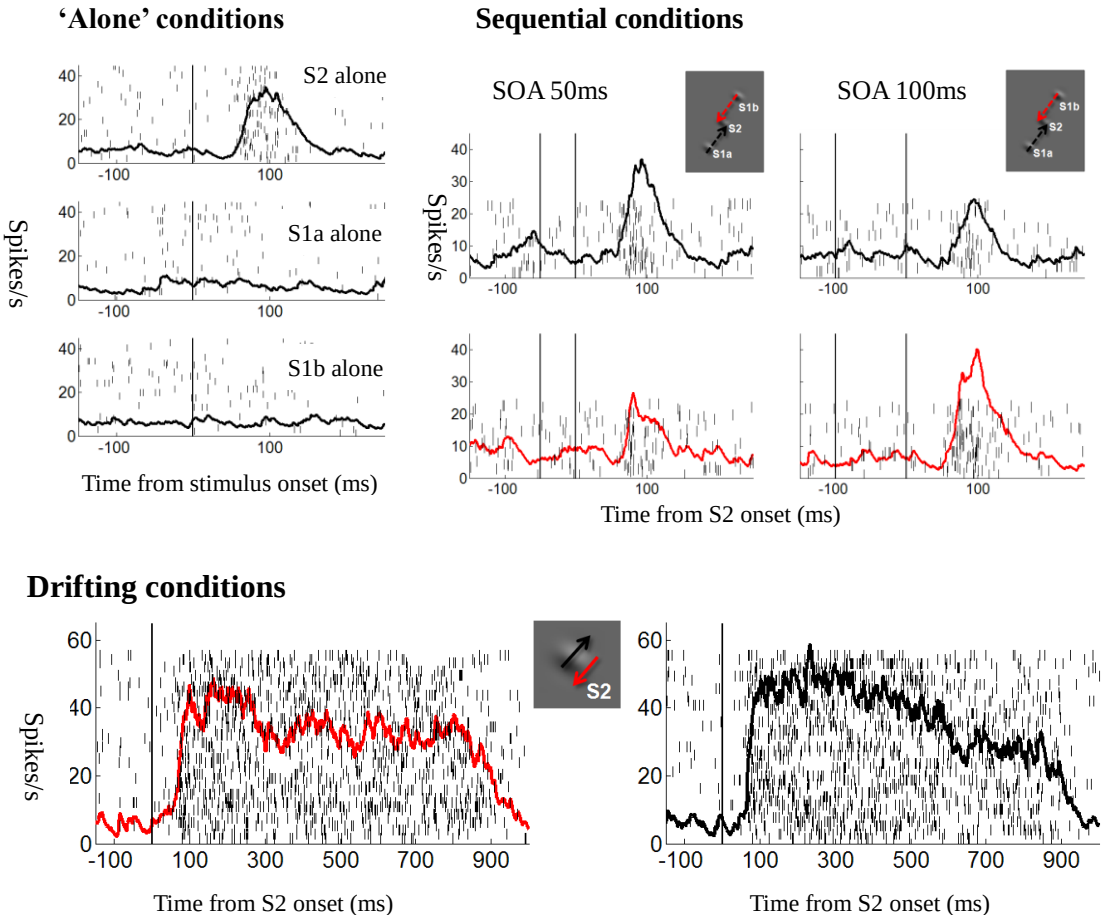

Figure 22. Raster plot of an example cell (#20130510-MUA).

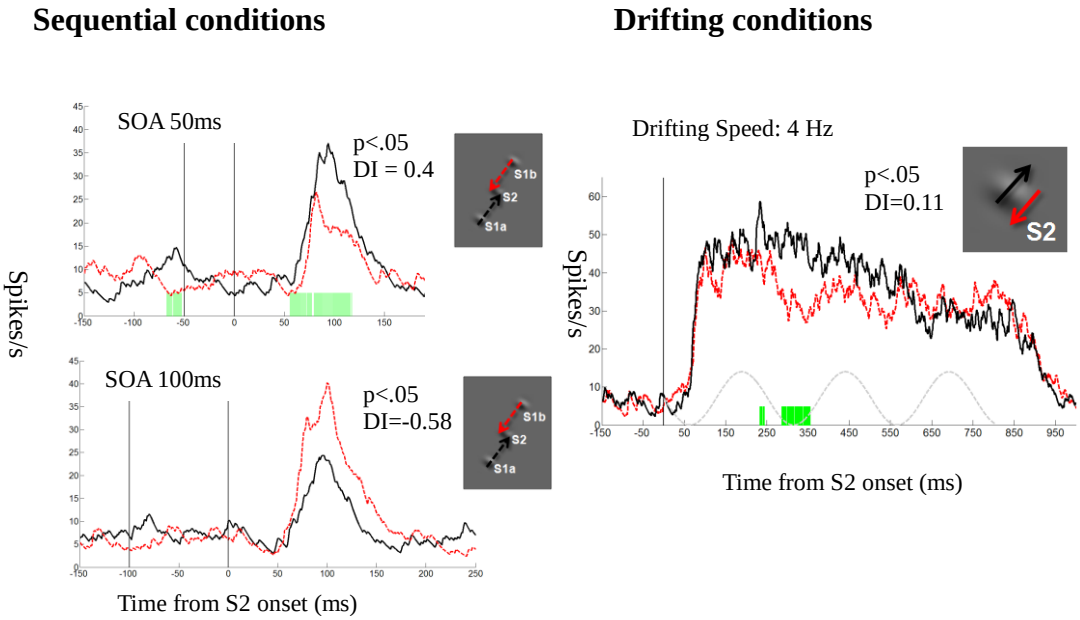

Figure 23. Comparison plot of an example cell (#20130510-MUA). DIs (direction selectivity index) were calculated with Eq.6-8, thus the DI of sequential conditions ranged from -1 to +1, yet the DI of drifting conditions ranged from 0 to +1.

The global DI was 0.4 with the SOA of 50ms, yet the global DI with the SOA of 100ms was -0.58. It represents that the directional preference for global direction reversed when the speed of global motion (varied by the SOAs) changed. The local DI was 0.11, and statistically significant with the duration of 250 ~350 ms after the S2 onset (t-test, p<.05).

3.3.3. Correlation analysis

3.3.3.1. Relationship between local and global directionalities

In this part, we summarize overall relationship between local and global directionalities using Pearson correlation analysis. We tested 62 units from 46 recording sessions. With the SOA of 50ms (Figure 24), a statistically significant positive correlation was found between local and global directionalities (r=.39, p<.01). These results suggest that V1 neurons tend to prefer the global motion direction that matched with their local directional preference.

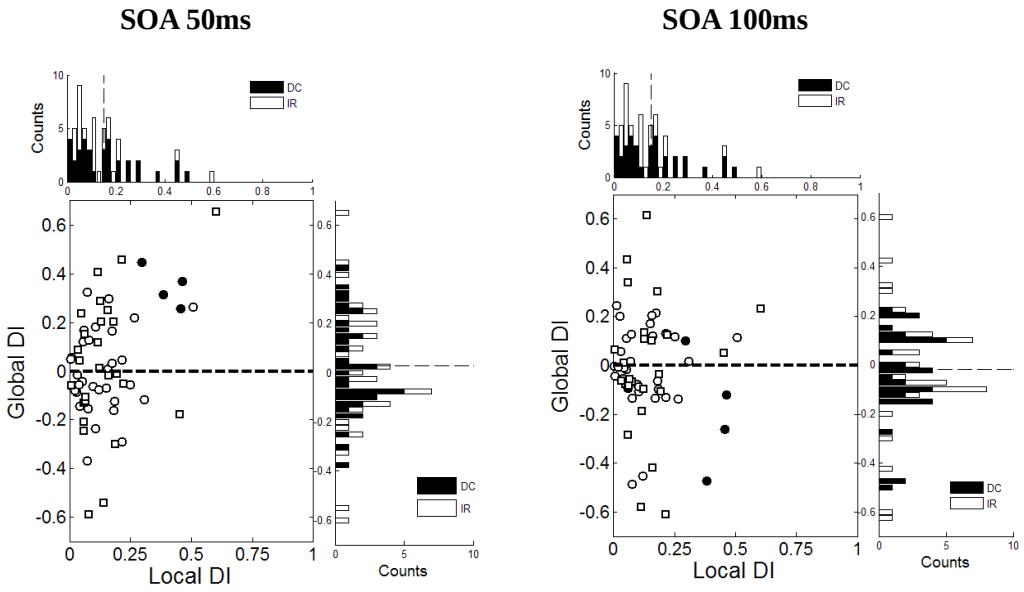

Figure 24. Summary scatter plot of two directionalities for 62 overall units (DC=36, IR=26). These results were calculated using Eq.6−Eq.8. Black filled symbols are simple (N=4) and open symbols are complex cells (N=58). Left plot shows the positive relationship between local and global directionalities for SOA of 50ms (r=.39, p<.01). DC and IR, resulted in r=.47 (p<.01) and r=.34 (p=.08), respectively. Right plot is for SOA of 100ms (r=−.04, p=.75). DC and IR, resulted in r=−.18 (p=.28) and r=.09 (p=.63) respectively. Circles for DC, squares for IR.

As previously stated, we calculated local and global directionalities by using an alternative method (described in method section [2.5.1]). In the SOA of 50ms, we found a significant positive correlation between local and global directionalities (r=.33, p<.01). Yet, there was not in the SOA of 100ms (r=-.11, p=.39). Regardless of whether a motion was local or global, a positive value indicates that a neuron preferred upward (or right) direction of motion, while a negative value represents a preference for downward (or left) direction.

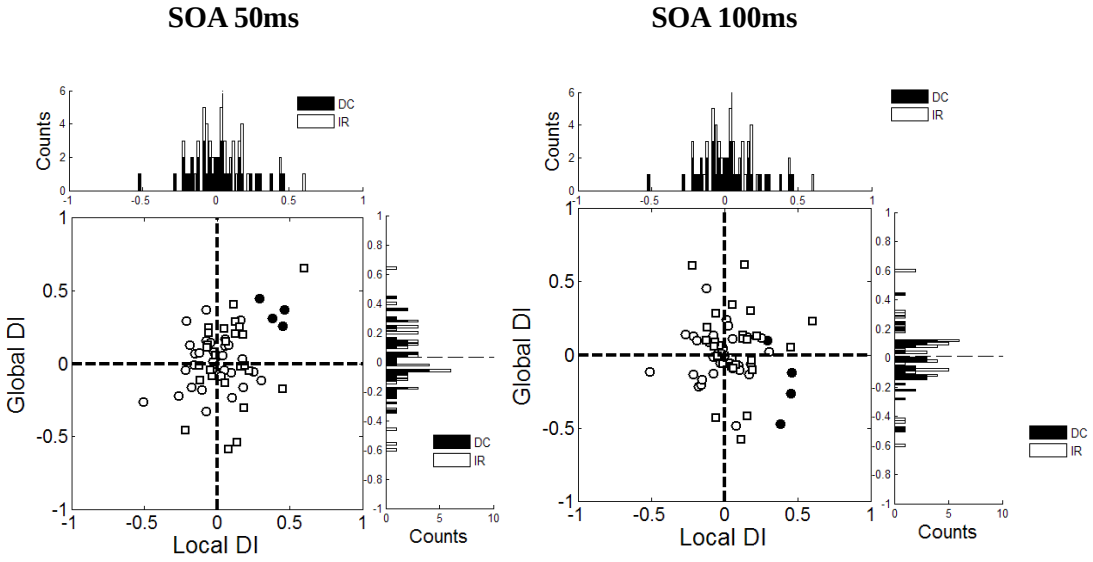

Figure 25. Summary scatter plots of two directionalities with an alternative calculation method for overall 62 units. Black filled symbols are simple cells (N=4). Open symbols are complex cells (N=58). These results were calculated using Eq.9−Eq.10, thus both local and global DI ranged from −1 to +1. A positive DI value indicates that the preferred direction was upward (or left). In contrast, a negative DI value represents the preferred direction was downward (or right). Left plot shows the positive relationship between local and global directionalities for SOA of 50ms (r=.33, p<.01). DC and IR, resulted in r=.42 (p<.01) and r=.27 (p=.17) respectively. Right plot is for SOA of 100ms (r=−.11, p=.39). DC and IR, resulted in r=−.22 (p=.18) and r=−.05 (p=.77) respectively.

3.3.3.2. Relationship between absolute values of local and global DI

After computing the absolute value of local and global DI which ranged from -1 to +1 (Eq. 9-10), we found that the local DI was positively correlated with the global DI. Significant positive correlation was found only with SOA of 50ms (Figure 26, r=.42, p<.01). Understandably, correlation analysis from local and global DIs with Eq.6-8 produced precisely the same result, since all DIs were calculated with the ratio [1-NP/P] for both DI calculation methods.

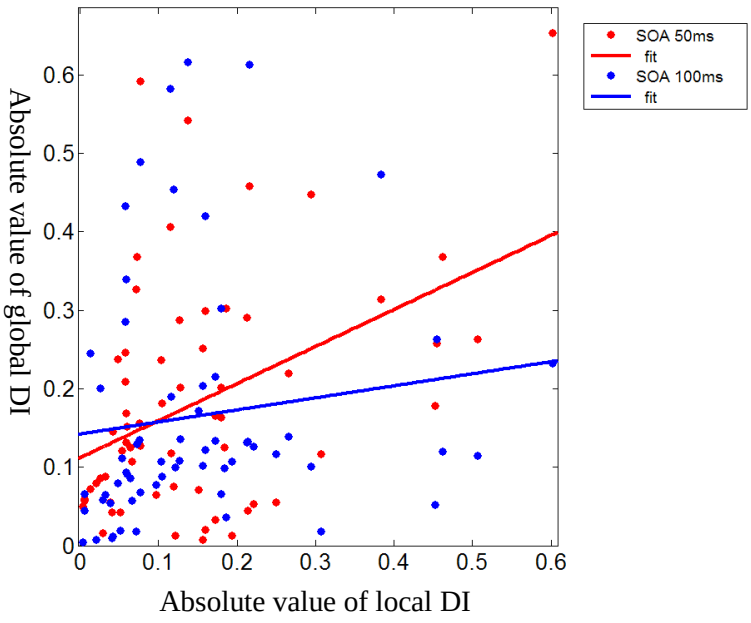

Figure 26. Correlation between absolute values of global and local DIs. Significant positive correlation was found between absolute values of local and global DIs (Only for SOA of 50ms, r=.42, p<.01).

3.4. Surround modulation index

The collinear S1 suppresses the spiking activity more than the parallel S1 does (Cavanaugh et al., 2001, Kim et al., 2012). However, in the current study, we did not test the collinear S1 due to making global apparent motion that matches to local motion. S1-S2 sequence always aligned with the axis that is orthogonal to their orientation, therefore, the orientations of S1 and S2 are always parallel to each other.

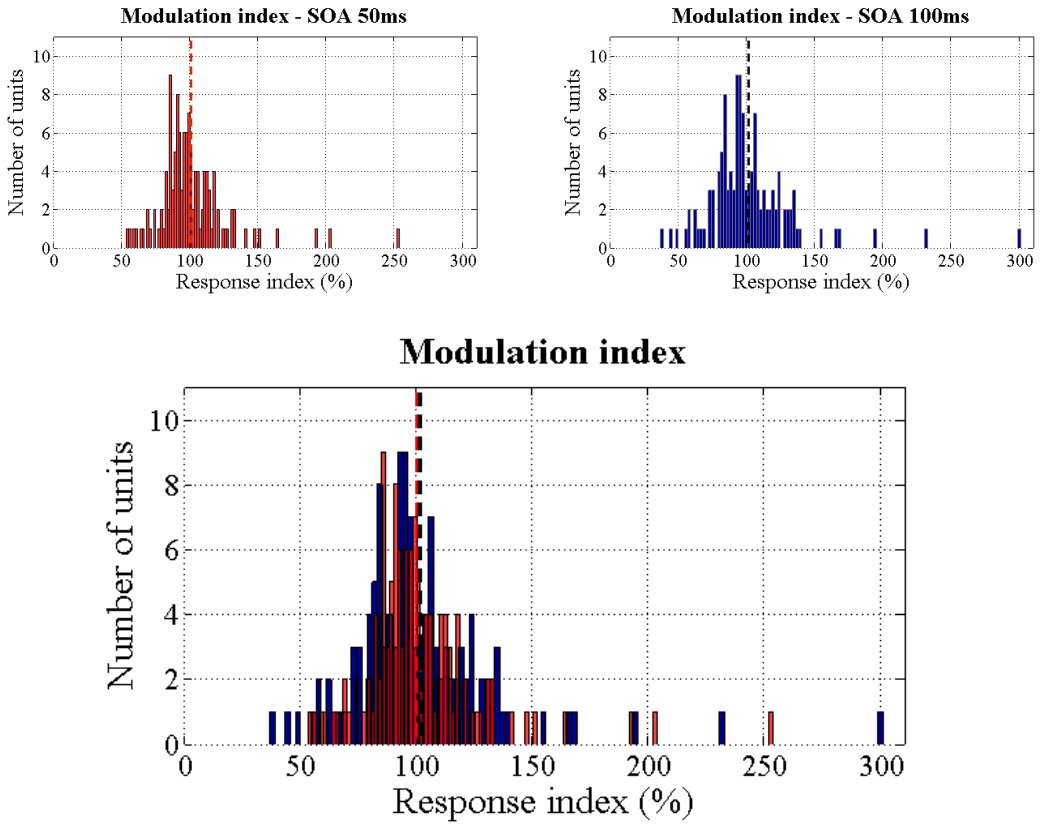

Figure 27. Distribution of response modulation index of two SOA conditions (N=62 units). Red for SOA of 50ms, Blue for SOA of 100ms.

Thus, the suppressive effect of the S1 was predicted to be weaker than previous studies due to its parallel configuration. Figure 27 illustrates the overall distribution of response modulation, and we calculated the response index (%) which means the relative activity of S1-S2 conditions to the activity of S2 alone condition (analysis window: 50-150ms after S2 onset). Therefore, 100% represents zero effect of the surround stimulus. We conclude that the surround effect was not more suppressive than facilitative with a statistical significance, although it tended to be slightly suppressive (the peak is slightly tilted to the left, suppressive zone).

3.5. Speed of local and global motion

We had the stimulus drifted at a speed ranging from 0.5 to 20 Hz. Hertz (Hz) is defined as the number of cycles per second, and it can be converted to the unit of degrees per second (υ) with a formula (13).

$$\upsilon = f * \lambda$$

deg per sec= (cycle per sec)*(1/cycle per deg) - (13)

After converting Hz to υ, we compared it with the speed of sequential stimuli conditions. In the case of drifting stimulus conditions, the maximum speed was 10 deg/s and the minimum was 0.03 deg/s (Figure 28, upper right panel). The speed of sequential conditions was much faster (maximum, 114 deg/s) than the speed of drifting conditions, and among all sequential stimuli (N=62), there were no cases which were slower than the speed of drifting stimulus.

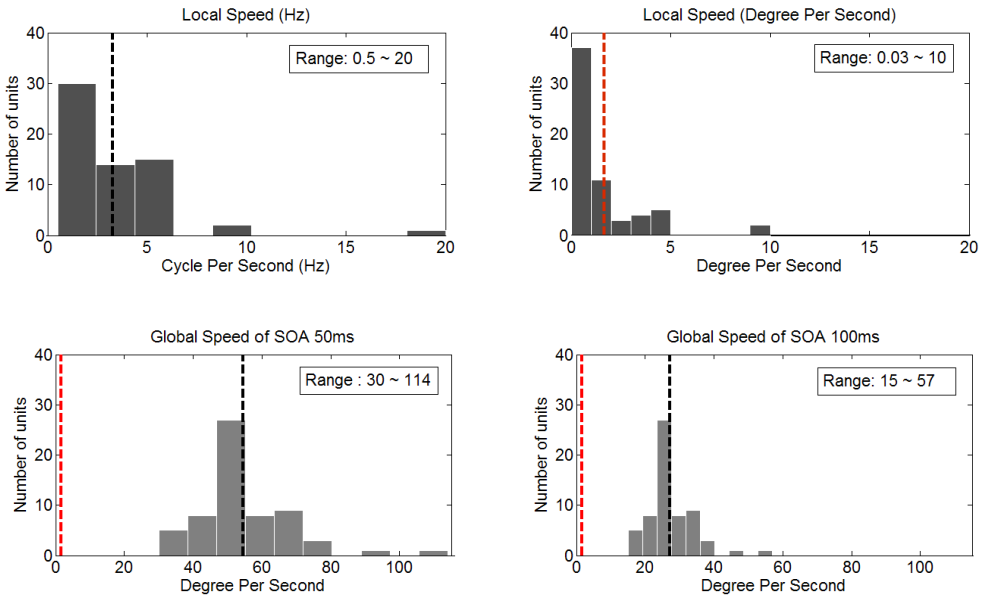

Figure 28. The distribution of speed for local (drifting) and global (sequential) conditions (N=62). Dashed-vertical line indicates a mean speed of all 62 units. In the figure for global speeds, the mean of local speed appears again (Red-dashed line) with the mean of global speed (Black-dashed line).

3.6. Local directionality index measured by the amplitude of first harmonic response

We calculated the Local DI based on the amplitude of first harmonic response instead of mean spike responses. As expected, overall DIs were higher than the DIs of mean spike responses.

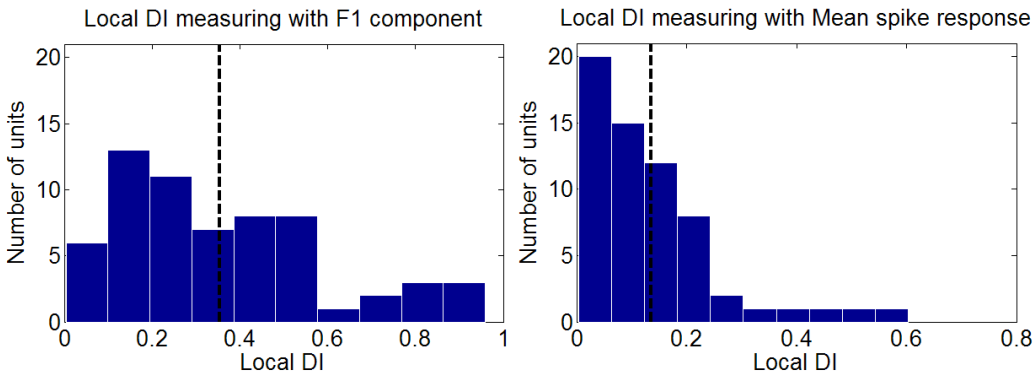

Figure 29. The distribution of local DI calculated by F1 component and mean spike response (N=62).

3.7. Eccentricity and cortical distance of surround stimulus

One of the most evident features of the primary visual cortex is an asymmetric cortical representation depending on eccentricity of stimulus. About half the surface area of the primary visual cortex represents the central 10° of the visual field (Horton, 2006). This property could contribute to the directional anisotropy in surround suppression reported in the current study. To examine this possibility, we analyzed the relationship between the difference in eccentricity of two surround stimuli and the global DI. Eccentricities of two S1 stimuli (S1a, S1b) varied across each recording session because orientation value determined the spatial arrangement of surround stimuli. Specifically, we computed cortical magnification eccentricity (CME) index for measuring the absolute difference of eccentricities of two S1 stimuli (S1a, S1b) in consideration of S2 eccentricity. Larger the CME index is, the more differences in eccentricity between two S1 stimuli.

$$\textbf{CME} = \frac{\textbf{abs}(\textbf{Eccentricity of S1a} - \textbf{Eccentricity of S1b})}{\textbf{Eccentricity of S2}} \quad -(14)$$

Figure 30 indicates that the CME index were unrelated to the absolute value of the global DI (SOA 50ms : r=-.05, p=.68, SOA 100ms : r=.16,p=.19).

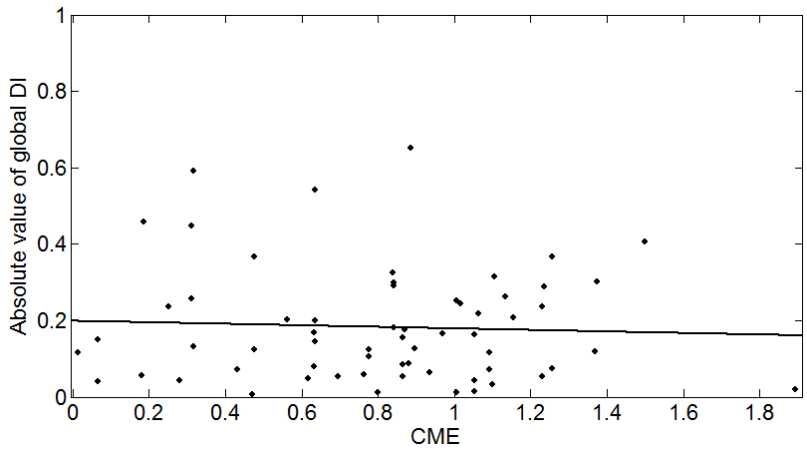

Figure 30. Correlation between the CME index and absolute global DI for SOA of 50ms (N=62). A large CME value indicates a large difference in eccentricity between two S1 stimuli. Each black circle represents each recording session and a black line is a linear regression for overall sessions. There was no significant relationship between the CME index and absolute global DI.

Although the eccentricity of stimulus represents a physical distance from the central fixation point in the visual field, visual space is anisotropically represented in the visual cortex. Thus, we tried to evaluate directional asymmetry with cortical distance between each S1 and S2. For this, we estimated cortical distance between S1 and S2 for each recording session as follows :

$$\mathbf{X = \lambda \ln (1 + E / E_0)} \qquad -(15)$$

$$\mathbf{Y = -\frac{\lambda E a \pi}{(E0+E)180^{o}}} \qquad -(16)$$

X and Y are cortical coordinates corresponding to locations in the retinotopic map of primary visual cortex (Dayan and Abbot, 2001). X values increase with the latitude coordinate which is the eccentricity 'E'. Y values vary with the the longitude coordinate which is the azimuth 'a'. These equations were obtained through information of cortical magnification factor (mm/deg), and for the macaque monkey, we used 12mm of λ and 0.75° of E_0 according to a previous study (Horton and Hoyt, 1991). For measuring relative cortical distances of two S1 stimuli from the S2 stimulus, we computed the ratio of two cortical distances and subtracted it from 1. We plotted it in the x-axis of Figure 31-A, and analyzed relationship with absolute value of global DI. There was no significant relationship (SOA 50ms : r=-.02, p=.84, SOA 100ms : r=.11,p=.38).

A. B.

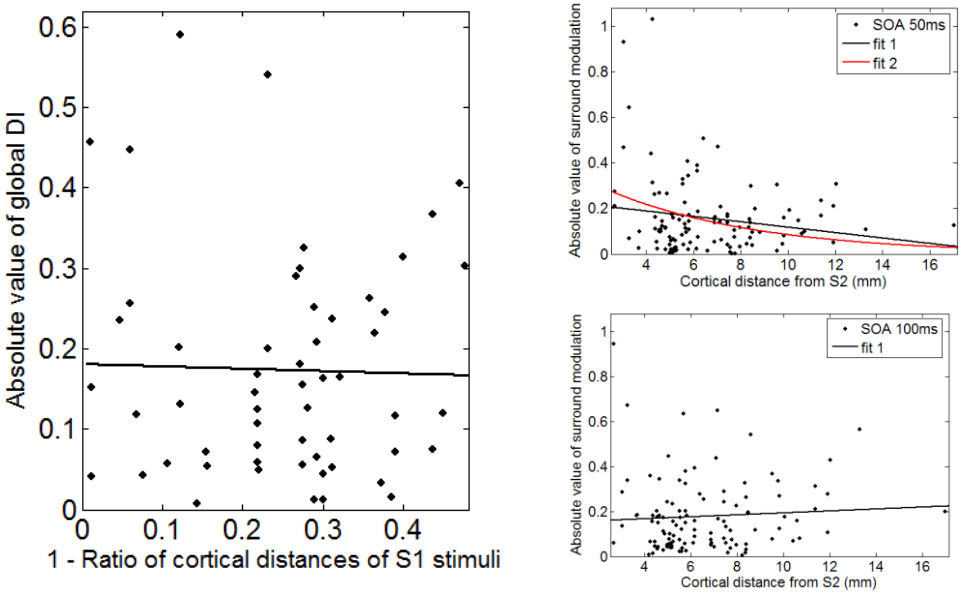

Figure 31. A. Correlation between the index for cortical distances of the S1 stimuli from the S2 and absolute global DI for SOA of 50ms (N=56, 6 were eliminated since the center of S1 stimuli was located in the opposite visual hemifield), which resulted in r=−.02, p=.84. A black circle represents each datum from each recording session. **B.** Cortical distance plotted against the absolute value of surround modulation (N=112). A black line is a fitting curve of linear regression, and a red line is a fitting curve of exponential function. For example, if the mean spike rate to S2 stimulus was 100 spike/s and the mean spike rate to S1 stimulus was 120 spike/s, the absolute value of surround modulation was 0.2.

Additionally, without taking the position of S1 stimulus into consideration, we examined whether the cortical distance of S1 from S2 predicted the strength of surround modulation (Figure 31-B and C). In other words, does cortically close S1 stimulus predict more surround modulatory effect than far S1 stimulus? There were no significant relationship between the cortical distance and absolute value of surround modulation (SOA 50ms : r=-.17, p=.06, SOA 100ms : r=.06, p=.49). Therefore, based on overall results in this section, we conclude that the directional asymmetry of spike response to S1-S2 sequence stimulus, i.e., global motion directionality, was not due to asymmetrical cortical magnification of separation between each S1 and S2.

4. Discussion

4.1. Global directionality

In the current study, we found that the spiking response to the RF stimulus (S2) was differentially modulated by the surround stimuli at two positions opposite from each other across the RF (S1a or S1b). This was observed in substantial number of neurons (32 units in SOA of 50ms, 39 units in SOA of 100ms, Table 3). Since rapid succession of these S1-S2 sequence stimuli elicits apparent motion, we contend that these results indicate that V1 neurons show a directional preference for global motion that encompasses both inside and outside the RF. These results are consistent with the previous study (Kim et al., 2012) that surround interaction in V1 is specific for spatial and temporal relation between S1 and S2. The match between the local and global directional preference found in the current study is new (Figure 24 and Figure 25). In figure 24, we operationally defined the global directionality that can have two signs (+ or -) depending on the consistency with the local directionality (Eq. 6-8). In figure 25, we also suggested new local and global DIs from an alternative method (Eq. 9-10), which both local and global DIs ranged from -1 to +1 regardless of their consistency (thus, whether a global DI had a positive or negative sign that was not dependent on a local DI). Despite the clear difference in the speed of stimulus motion between sequential and drifting stimulus conditions (Figure 28), some neurons preferred global direction that matched with their local directional preference. The overall scatter plot between the two directionalities with a significant correlation coefficient ($r=.39$, $p<.01$, Figure 24) indicate that the relationship was not observed by chance. Also, a significant positive correlation was found between two directionalities from an alternative method ($r=.33$, $p<.01$, Figure 25), too. From these result, both directionality calculation methods

were effective way to measure the significant positive relationship between two directional preferences. Similarly, the absolute value of global DI was significantly correlated with the absolute value of local DI ($r=.42$, $p<.01$). These results indicate that the neurons highly sensitive to local direction are also quite sensitive to spatiotemporal stimulus sequence beyond its cRF (Figure 26).

Stimulus onset asynchrony (SOA) was also a matter of consideration. Despite the similarity of modulation index (Figure 27) between two SOA conditions, there were systematic differences in the magnitude of correlation between the local and global DIs (Figure 24 and Figure 25). The positive relationship between the global DI and the local DI was only found in SOA of 50ms, suggesting that a fine-tuned surround interaction enabled V1 neurons to signal the speed of global motion. Previous studies (Muller et al., 2003; Kim et al., 2012) observed that the effect of surround was diminished at around 100ms of SOA. Therefore, we conclude that the global DI for SOA of 50ms was significantly correlated with local DI with the aid of surround interaction.

4.2. Sequential stimuli as a global motion stimulus

An important aspect of this study is that we tested global directions with sequential stimuli that were composed of two focal Gabor stimuli. By adopting short temporal intervals (50 or 100ms) and short distances (1.5 cRF diameters) between centers of two Gabor stimuli, we created apparent motion stimulus not encroaching on the boundaries of the cRF. On the other hand, many other studies generally used a drifting bar or annuli or full-field surround stimulus for generating surround modulation effect (Bair et al., 2003; Guo et al., 2006; Henry et al., 2013). Another difference between our study and the study of Guo et al. (2006) is that whereas they matched the speed of drifting bar with the neuron's preferred temporal frequency, we did not match the speed of global with local

motion. Since we aimed at making apparent motion stimulus without loss of surround modulatory effect, it was inevitable to use short temporal intervals (50 or 100ms) instead of using optimal temporal frequency. Regardless of large speed differences between local and global motion (Figure 28), overall trend suggests that the V1 neuron tend to prefer specific global direction, which matched the preferred direction of local motion (Figure 24 and Figure 25). From these facts we deduced that short SOAs (50 or 100ms) could make the sequential stimuli more realistic motion stimulus, suggesting feedback connections that has an effect on neurons of V1.

4.3. Analysis period for calculating the mean response

In the case of complex cells in our dataset, we calculated the mean spike density during the period of 50-150ms after RF target onset for sequence, and 50-800ms for drifting. Whereas the mean densities of complex cells were robust regardless of the analysis period within drifting duration, the amplitude of F1 component of simple cells differed by the analysis period. Therefore, there is a need to compare the amplitude of F1 component from different methods (ex. Fourier analysis, sine-wave fitting, peak-to-peak), also switching from one type of period (ex. from 50ms ~ to 1 cycle) to other types of period (ex. from 100ms ~ to 2 cycles). In the current study, we used Fourier analysis window from 150 to 900 ms for 4Hz stimulus, thus measuring the amplitudes of 3 cycles. On the other hand, we used window from 50 to 250 ms for 5Hz stimulus, which contained 1 cycle.

4.4. Low proportion of simple cell & directional cell

From the Figure 16, we speculated about the reasons for the low proportion of simple

cell (F1/F0>1) in the current study (N=4). Spiking responses well followed the temporal frequency of drifting stimulus until 1 cycle/deg. Spatial frequencies higher than 1 cycle/deg eliminated the pattern of phase-locked response to 4Hz drifting stimulus. Since we did not choose the spatial frequency based on the amplitude of F1 component in the mapping stage, there were some cells that lost their simple cell behavior by stimulus chosen during the main experiment.

Most of cells (96%, 60 units except for 2 units) were defined as non-directional on the basis of classic criterion (local DI<0.5). However, our drifting stimulus confined within the cRF (mean diameter = 1.8 deg), unlike other studies (Livingstone, 1998; Priebe and Ferster, 2005) that used full field stimulus, might have underestimated direction selectivity. Kim et al. (2007) also determined direction selectivity with 3-5 deg cosine grating. Another possible cause is the type of stimulus for testing directionality. Most other studies used optimally oriented sinusoidal gratings (Cavanaugh et al., 2002; Priebe and Ferster, 2005; Peterson et al., 2006; Guo et al, 2006) or optimally oriented single bar stimuli (Conway and Livingstone, 2003) or cosine grating (Kim et al., 2007) for measuring direction selectivity, in contrast, we measured directionality index using Gaussian filtered Gabor stimuli with 64% contrast (Eq.1-2).

4.5. Implications for motion processing

Whereas previous studies have focused on the neural mechanism of direction selectivity of V1 neurons (Livingstone, 1998; Priebe and Ferster, 2005), here we are more concerned with the relation to global motion processing. According to Priebe and Ferster (2005), directionality is produced by both excitatory and inhibitory synaptic current in the tuned direction. This may be compatible with both facilitative and suppressive surround interaction (Kim et al., 2012). In addition, the current study is deviated from a traditional

concept of global motion integration; rather than focusing on pattern/component classification within cRF (Movshon et al., 1986; Guo et al., 2004; Majaj et al., 2007), we focused on the motion integration extending beyond the cRF.

The limited role of the area MT for global motion processing was repeatedly reported (Majaj et al., 2007; Hedges et al., 2011), suggesting local motion information inside cRF was not properly integrated within cRF of MT neuron. The pattern selectivity of MT neuron was present only when two gratings overlapped within cRF, yet disappeared when the two gratings separately presented as local patches within cRF (Majaj et al., 2007). Thus, it is questionable whether the area MT is an anatomical site of integration for global motion. In the current study, in the area V1, inhomogeneous subthreshold responses from the surround zone (S1a or S1b) made asymmetric response depending on stimulus direction, consistent with a previous study (Kim et al., 2012). Therefore, this study provided new insights into the role of the area V1 for global motion processing.

References

Adams, D. L., Economides, J. R., Jocson, C. M., and Horton, J. C. (2007). A biocompatible titanium headpost for stabilizing behaving monkeys. *J Physiol 98*:993-1001.

Adelson, E. H., and Bergen, J. R. (1985). Spatiotemporal energy models for the perception of motion. *J. Opt. Soc. Am. A. 2*: 284–299.

Albright, T. D. (1984). Direction and orientation selectivity of neurons in visual area MT of the macaque. *J Neurophysiol 52*: 1106-1130.

Bair, W., Cavanaugh, J. R., and Movshon, J. A. (2003). Time course and time-distance relationships for surround suppression in macaque V1 neurons. *J Neurosci 23*: 7690–7701.

Born, R. T., and Bradley, D. C. (2005). Structure and function of visual area MT. *Annu. Rev. Neurosci.*
*2005. 28:*157–89

Bringuier, V., Chavane, F., Glaeser, L., and Fregnac, Y. (1999). Horizontal propagation of visual activity in the synaptic integration field of area 17 neurons. *Science* (New York, NY 283:695-699)

Cavanaugh, J. R., Bair, W., and Movshon, J. A. (2002). Nature and interaction of signals from the receptive field center and surround in macaque V1 neurons. *J. Neurophysiol. 88*: 2530–2546.

Cavanaugh, J. R., Bair, W., and Movshon, J. A. (2002). Selectivity and spatial distribution of signals from the receptive field surround in macaque V1 neurons. *J Neurophysiol 88*: 2547–2556.

Conway, B. R., and Livingstone, M. S. (2003). Space-time maps and two-bar interactions of different classes of direction-selective cells in macaque V1. *J Neurophysiol 89*: 2726–2742.

Dayan, P., and Abbot, L. F. (2001). Theoretical neuroscience. (The MIT press)

Guo, K., Benson, P.J., and Blakemore, C. (2004). Pattern motion is present in V1 of awake but no anaesthetized monkeys. *Eur J Neurosci 19*:1055–1066.

Guo, K., Robertson, R. G., Nevado, A., Pulgarin, M., Mahmoodi, S., and Young, M. P. (2006). Primary visual cortex neurons that contribute to resolve the aperture problem. *Neuroscience 138:* 1397-1406

Guo, K., Robertson, R. G., Pulgarin, M., Nevado, A., Panzeri, S., Thiele, A., Young, M. P. (2007). Spatio-temporal prediction and inference by V1 neurons. *Eur J Neurosci 26*0: 1045-1054.

Gur, M., Kagan, I., and Snodderly, D. M. (2005). Orientation and direction selectivity of neurons in V1 of alert monkeys: Functional relationships and laminar distributions. *Cerebral Cortex 15*: 1207-1221.

Gur, M., and Snodderly, D. M. (2007). Direction selectivity in V1 of alert monkeys:

evidence for parallel pathways for motion processing. *J Neurophysiol 585.2* : 383-400.

Hedges, J. H., Gartshteyn, Y., Kohn, A., Rust, N. C., Shadlen, M. N., Newsome, W. T., and Movshon, J. A. (2011). Dissociation of neuronal and psychophysical responses to local and global motion. *Current Biology 21*: 2023-2028.

Henry, C. A., Joshi, S., Xing, D., Shapley, R. M., and Hawken, M. J. (2013). Functional characterization of the extraclassical receptive field in macaque V1: contrast, orientation, and temporal dynamics. *J. Neurosci. 33(14):* 6230-6242

Horton, J. C., and Hoyt, W. F. (1991). The representation of the visual field in human striate cortex: A revision of the classic Holmes map. *Arch Ophathalmol (109)* : 816-824.

Horton, J. C. (2006). Ocular integration in the human visual cortex. *Can J Ophthalmol (41)* : 584-593

Kim, H. (2007). Information of sacaddic direction in postsaccadic discharge in the primate V1 neurons. *M.S. thesis. Seoul National University.*

Kim, T., Kim, H.R., Kim, K., and Lee, C. (2012). Modulation of V1 spike response by temporal interval of spatiotemporal stimulus sequence. *PLoS ONE 7(10):* e47543

Kim, T. (2008). Response selectivity of V1 neurons for spatiotemporal sequence of stimulus orientation. *M.S. thesis. Seoul National University.*

Lee, J. (2008). Activity of the primate V1 neurons in visual detection tasks: neural and behavioral variabilities. *PhD thesis. Seoul National University.*

Lewicki, M. S. (1998). A review of methods for spike sorting: the detection and classification of neural action potentials. *Network 9(4)*: R53-78.

Livingstone, M. S. (1998). Mechanisms of direction selectivity in macaque V1. *Neuron 20:* 509-526.

Majaj, N. J., Carandini, M., and Movshon, J. A. (2007). Motion integration by neurons in macaque MT is local, not global. *J. Neurosci. 27*: 366–370.

Marr, D. (1982). Vision (New York: W.H. Freeman & Co.).

Movshon, J. A., Adelson, E. H., Gizzi, M. S., and Newsome, W. T. (1986). The analysis of moving visual patterns. *Exp. Brain Res 11*:117–151.

Muller, J. R., Metha, A. B., Krauskopf, J., and Lennie, P. (2003). Local signals from beyond the receptive fields of striate cortical neurons. *J Neurophysiol 90*: 822–831.

Pack, C. C., Livingstone, M. S., Duffy, K. R., and Born, R. T. (2003). End-stopping and aperture problem: two-dimensional motion signals in macaque V1. *Neuron 39:* 671-690

Peterson, M. R., Li, B., and Freeman, R.D. (2004). The derivation of direction selectivity in the striate cortex. *J. Neurosci. 24(14):* 3583-3591.

Peterson, M. R., Li, B., and Freeman, R.D. (2006). Direction selectivity of neurons in the striate cortex increases as stimulus contrast is decreases. *J Neurophysiol. 95:* 2705-2712.

Priebe, N. J., Mechler, F., Carandini, M., and Ferster, D. (2004). The contribution of spike threshold to the dichotomy of cortical simple and complex cells. *Nat. Neurosci.7*: 1113–1122.

Priebe, N. J., and Ferster, D. (2005). Direction selectivity of excitation and inhibition in simple cells of the cat primary visual cortex. *Neuron 45:* 133-145

Priebe, N. J., and Ferster, D. (2008). Inhibition, spike threshold, and stimulus selectivity in primary visual cortex. *Neuron 57*:482-497.

Rivlin-Etzion, M., Wei, W., and Feller, M. B. (2012). Visual stimulation reverses the directional preference of direction-selective retinal ganglion cells. *Neuron 76:* 518-525

Rodman, H. R., and Albright, T. D. (1989). Single-unit analysis of pattern-motion selective properties in the middle temporal visual area (MT). *Exp Brain Res 75*: 53-64

Rodman, H. R., Albright, T. D. (1987). Coding of visual stimulus velocity in area MT of the macaque. *Vision Res 27:* 2035-2048.

Saul, A. B, and Humphrey, A. L. (1990). Spatial and temporal response properties of lagged and nonlagged cells in cat lateral geniculate nucleus. *J Physiol 64*: 206–224.

Saul, A. B., and Humphrey, A. L. (1992). Evidence of input from lagged cells in the lateral geniculate nucleus to simple cells in cortical area17 of the cat. *J Physiol 68*: 1190–1208.

Series, P., Lorenceau, J., and Fregnac, Y. (2003). The “silent” surround of V1 receptive

fields: theory and experiments. *J Physiol 97:*453-474.

Simoncelli, E. P., and Heeger, D. (1998). A model of neuronal responses in visual area MT. *Vision Res 38:* 743-761.

Skottun, B. C., De Valois, R. L., Grosof, D. H., Movshon, J. A, Albrecht, D. G and Bonds, A. B. (1991). Classifying simple and complex cells on the basis of response modulation. *Vision Res 31*:1079–1086.

Thompson, K. G., Hanes, D. P., Bichot, N. P and Schall, J. D. (1996). Perceptual and motor processing stages identified in the activity of macaque frontal eye field neurons during visual search. *J. Neurophysiol. 76* : 4040–4055.

Vinje, W. E., and Gallant, J. L. (2002). Natural stimulation of the nonclassical receptive field increases information transmission efficiency in V1. *J. Neurosci. 22*: 2904–2915.

Young, M. P. (2000). The architecture of visual cortex and inferential processes in vision. *Spat Vis 13:* 137-146

Yu, A. J. (1999). Classification of extracellular microelectrode recordings from the human brain. *Caltech Summer Undergraduate Research Fellowship.*

국문 초록

일차시각피질(V1)의 뉴런들은 전통적인 수용장(the classical receptive field) 내부에 제시되는 시각정보들을 처리한다. 이 국지적인 정보(local information)들은 수용장을 넘어서는 광역적인 시각 특징(global visual features)들을 복원하기 위해 V1의 다음 단계들에서 수용장 바깥의 정보들과 통합된다고 생각되어 왔다. 그러나 V1에서도 수용장 바깥에 제시되는 자극에 의해 신경세포의 활동이 조절된다는 사실이 알려져 왔다. 같은 맥락에서, 수용장을 넘어서서 순차적으로 제시되는 시공간 자극의 제시 간격에 의해 활동이 조절된다는 사실이 보고되었다(Kim et al., 2012). 이러한 사실들은 V1 뉴런들이 수용장을 넘어서는 광역운동(global motion)의 처리에 참여하고 있음을 시사하고 있다.

본 연구는 V1 뉴런들이 수용장을 넘어서는 광역운동에 대해 방향선호성(directional preference)을 보이는지, 또 이러한 방향선호가 미세한 주변상호작용(surround interaction)을 기반으로 발생하는 현상인지 알아보고자 하였다. 구체적으로, 순차적인 두 개의 정지된 가보 자극(stationary Gabor stimuli)을 사용하여 광역적 방향선호성(global directional preference)을 측정하였다. 순차적인 두 가보 자극 가운데 먼저 제시되는 자극('S1')이 우선 수용장 외부에 제시되고 난 후, 50ms 또는 100ms의 시간간격(stimulus onset asynchrony; SOA)을 두고 두 번째 자극('S2')이 수용장 내부에 제시된다. S1은 S2가 제시되기 전에 수용장의 두 측면 중 한 측면에 제시되었다. 그러므로, 두 측면 중 어떤 측면에 S1 이 제시되었는지에 따라 순차 자극의

두 가지 반대되는 운동 방향이 만들어졌다. 그리고 이러한 방식으로 측정된 광역적 방향선호성을 국지적 방향선호성(local directional preference)과 비교하였다. 국지적 방향선호성은 수용장 내부에 두 반대 방향으로 움직이는 가보자극을 제시함으로써 측정하였다. 광역적 방향선호 조건에서, S1의 제시 위치를 달리하여 수용장을 넘어서는 두 가지 서로 다른 운동방향을 만들어 낸 것과 달리, 국지적 방향선호 조건에서는 세포가 선호하는 자극의 기울기(orientation)에 직교하는 두 가지 축을 따라 두 가지 운동방향이 수용장 내부에서 비교되었다.

연구 결과, S1을 단독으로 제시하는 경우에는 뉴런의 활동전위(action potentials or spikes)가 일어나지 않음에도 불구하고, S2에 대한 뉴런의 반응은 S1에 의해 유의미하게 조절되었다. 이 결과는 기존의 보고(Kim et al., 2012)와 일치한다. 순차 자극의 제시 방향에 따라 S2에 대한 반응을 조절하는 정도가 비대칭적이었는데, 이 결과는 수용장을 넘어서는 S1-S2로 구성된 가현운동(apparent motion)에 대한 방향선호를 의미한다. 그리고 광역적 방향선호성과 국지적 방향선호성간의 유의미한 정적 상관관계가 발견되었는데, 이는 V1 뉴런들이 선호하는 국지적 방향과 일치되는 광역적 방향을 더 선호하는 경향이 있음을 시사한다. 정적 상관은 SOA가 50ms인 조건에서만 발견되었고 SOA가 100ms인 조건에서는 발견되지 않았다. 이러한 결과들은 V1 뉴런들이 광역 운동정보의 처리에 참여하고 있으며, 이 처리가 주변 상호작용(surround interaction)에 기초하고 있음을 시사한다. 그리고 이 주변 상호작용은 중심자극(center stimulus, 'S2')과 주변자극(surround stimulus, 'S1') 간의 시공간적 관계에 따라 미세하게 조정되고 있음을 나타낸다.

주요어 : 주변 상호작용, 수용장, V1, 광역운동, 방향선호성, aperture problem

학번 : 2011-20118